Title

Climate Warming Alters Nutrient Storage in Seasonally Dry Forests: Insights From a 2,300 m Elevation Gradient

Journal

Global Biogeochemical Cycles, 36(11)

ISSN

0886-6236

Authors

Yang, Yang
Berhe, Asmeret Asefaw
Barnes, Morgan E
et al.

Publication Date

2022-11-01

DOI

10.1029/2022gb007429

Climate Warming Alters Nutrient Storage in Seasonally Dry Forests: Insights from a 2300 m Elevation Gradient

Yang Yang[1], Asmeret Asefaw Berhe[1,2], Morgan E. Barnes[2,3], Kimber C. Moreland[2,4], Zhiyuan Tian[5,7], Anne E. Kelly[6,8], Roger C. Bales[1], Anthony T. O'Geen[7], Michael L. Goulden[8], Peter Hartsough[7], Stephen C. Hart[1,2]

[1]Sierra Nevada Research Institute, University of California, Merced, CA, USA

[2]Department of Life and Environmental Sciences, University of California, Merced, CA, USA

[3]Pacific Northwest National Laboratory, Richland, WA, USA

[4]Lawrence Livermore National Laboratory, Livermore, CA, USA

[5]Institute of Soil Sciences, Chinese Academy of Sciences, Beijing, China

[6]The Nature Conservancy, AK, USA

[7]Department of Land, Air, and Water Resources, University of California, Davis, CA, USA

[8]Department of Earth System Science, University of California, Irvine, CA, USA

Corresponding author: Yang (yyang103@ucmerced.edu; Orcid ID: 0000-0002-2760-0992)

Key points

1. In Mediterranean-climate regions, warming will decrease forest storage of C, N, and P at warmer sites but not at colder sites
2. Climatic impacts on soil C storage can remain substantial even in deep soil and weathered bedrock
3. Ecosystem C residence times will decrease with rising air temperatures but will increase with major droughts

This article has been accepted for publication and undergone full peer review but has not been through the copyediting, typesetting, pagination and proofreading process, which may lead to differences between this version and the Version of Record. Please cite this article as doi: 10.1029/2022GB007429.

Abstract

Understanding potential response of forest carbon (C) and nutrient storage to warming is important for climate mitigation policies. Unfortunately, those responses are difficult to predict in seasonally dry forests, in part, because ecosystem processes are highly sensitive to both changes in temperature and precipitation. We investigated how warming might alter stocks of C, nitrogen (N), and phosphorus (P) in vegetation and the entire regolith (soil + weathered bedrock or "saprock") using a space-for-time substitution along a bioclimatic gradient in the Sierra Nevada, California. The pine-oak and mixed-conifer forests between 1160 – 2015 m elevation have more optimal climates (not too dry or hot) for ecosystem productivity, soil weathering, and cycling of essential elements than the oak savannah (405 m) and subalpine forest (2700 m). We found decreases in overstory vegetation nutrient stocks with decreasing elevation because of enhanced water limitation and greater occurrence of disturbances. Stocks of C, N, and P in the entire regolith peaked at the pine-oak and mixed-conifer forests across the bioclimatic gradient, driven by thicker regolith profiles and greater nutrient input rates. These observations suggest long-term warming will decrease ecosystem nutrient storage at the warmer, transitional pine-oak zone, but will increase nutrient storage at the colder, subalpine zone. Assuming steady-state conditions, we found the mean residence time of ecosystem C decreased with projected rising air temperatures and increased following a major drought event across the bioclimatic gradient. Our study emphasizes potentially elevation-dependent changes in nutrient storage and C persistence with warming in seasonally dry forests.

Plain Language Summary

Carbon accumulation in forest ecosystems is a promising natural climate solution to offset rising temperatures. However, major knowledge gaps exist on warming impacts on carbon storage in seasonally dry forests, where ecosystem processes are highly sensitive to both changes in temperature and precipitation. We investigated nutrient pools in vegetation, soil, and weathered bedrock along a 2300-m bioclimatic gradient in the Sierra Nevada, California. We observed unimodal changes in ecosystem

nutrient stocks with decreasing elevation, suggesting long-term warming will decrease nutrient storage at relatively warm sites (e.g., transitional pine-oak zone), but will increase nutrient storage at cold sites (e.g., subalpine zone). Deep soil and weathered bedrock respond to a changing climate similarly to surficial soils, demonstrating the importance of accounting for deep carbon to accurately assess carbon turnover rates. Estimated average time (assuming steady-state) that a carbon atom resides in forests from initial photosynthetic fixation until respiration loss increases with projected rising air temperatures and decreases following a major drought event, which emphasizes the complex response of carbon storage to warmer and drier conditions. Our study provides a broader understanding of how ecosystem structure and function may respond to warming in Mediterranean-climate regions, some of the most vulnerable to climate change.

1 Introduction

The world's forest ecosystems store considerable amounts of carbon (C), and removed ~30% of annual fossil fuel emissions from 2009 to 2018 (Dixon et al., 1994; Friedlingstein et al., 2019; Harris et al., 2021; Pan et al., 2011). Therefore, forest C accumulation has been proposed as an important natural climate solution, and forest C pools have been used in ecosystem models for developing climate mitigation policies. However, forest C cycle is sensitive to a changing climate and will be altered by the rising air and soil temperatures (Giorgetta et al., 2013; Zhang et al., 2016). Accurate C storage forecasts depend on an understanding of warming impacts on forest ecosystems.

Regions experiencing Mediterranean climates, found on western coasts of continents roughly between 30° and 45° latitude north and south of the equator, have strong seasonal and interannual variability in precipitation (Deitch et al., 2017; Seager et al., 2019). The temporal asynchrony of warm temperatures and moist conditions constrain biological and geochemical activity, except during spring and fall when both temperature and moisture are co-limiting (Hart et al., 1992; van der Molen et al., 2011). These climatic controls, along with the extent by which air temperature and precipitation are predicted to change as the Earth continues to warm, have resulted in some researchers classifying these climatic regions as climate change "hot-spots," defined as a region whose climate is especially responsive to global change (Giorgi, 2006; Lionello, 2012; Lionello & Scarascia, 2018). Excessive warming in these regions increases the magnitude and duration of precipitation deficits, which can have catastrophic effects on ecosystem productivity and services (Diffenbaugh et al., 2015; Lund et al., 2018). Little is known how future warmer and drier conditions might alter forest C pools in these seasonally dry regions (Prichard et al., 2021; Siyum, 2020).

The availability of soil nitrogen (N) and phosphorus (P) constrains forest C storage by influencing biological activity such as growth, mortality, and decomposition rates (Campo, 2016; Maaroufi & De, 2020; Terrer et al., 2019). In most forests, soil N originates primarily from biological N fixation and atmospheric deposition, and is found mostly in organic forms. Nitrogen becomes available to most plants only after microorganisms decompose the organic compounds, releasing inorganic N into the soil solution

(Boring et al., 1988; Gower, 2003; McGill & Cole 1981). Soil P originates primarily from mineral weathering of the parent material and atmospheric deposition, and is found in both organic and inorganic forms. Most soil P is unavailable for plant uptake because it exists in organic forms, precipitates with calcium or aluminum, or is strongly sorbed to minerals (e.g., aluminum and iron oxides; Gu et al., 2020; Walker & Syers, 1976; Wood et al., 1984). In seasonally dry forests, nutrient cycling processes are sensitive to changes in temperature and precipitation (Allen et al., 2017; Berner et al., 2017; Serrano-Ortiz et al., 2015). Thus, climate warming will impact the amount of total and available N and P in soils (Hou et al., 2018; Yang et al., 2022), indirectly influencing ecosystem productivity and C storage.

Carbon residence time determines the C storage in forests, but its response to climate warming remains unclear. The mean residence times of ecosystem C (MRT, the mathematical inverse of mean turnover rate) is defined as the average time a C atom resides in an ecosystem, from the initial fixation of carbon dioxide from the atmosphere during photosynthesis until its loss from the ecosystem back to the atmosphere primarily by respiration (Barrett, 2002). However, current estimates of the MRTs are often based on C stocks of near-surface horizons (typically just the upper 30 cm of the regolith profile, e.g., Berner et al., 2017; Carvalhais et al., 2014; Yan et al., 2017). Carbon stored in subsoil horizons and materials below soil such as saprock (defined as weathered bedrock where the structure of the rock is maintained but its mechanical strength is considerably reduced; Graham et al., 2010) can accumulate up to 70% of total regolith C (Jobbágy & Jackson, 2000; Moreland et al., 2021). The large amount of C stored in deep soil and saprock, similar to surficial soils, are responsive to rising temperatures (Gross & Harrison, 2019; Hicks Pries et al., 2017; Li et al., 2020; Soong et al., 2021). Studies exploring the entire regolith will improve the understanding of ecosystem responses to warming.

Our current knowledge of warming-associated changes in nutrient pools and turnover is primarily derived from manipulative studies, and therefore limited to relatively short time periods (i.e., less than one decade, Lu et al., 2013; Melillo et al., 2011; Rustad et al., 2001). These transient, shorter time-scale responses may not be representative of warming impacts in forest ecosystems, where vegetation is long-lived, and soils form slowly (Melillo et al., 2017). Observations from manipulative experiments alone are

also insufficient to help predict forest nutrient storage under climate warming because models are often simulated at multidecadal time scales (Friedlingstein et al., 2014; Luo et al., 2008; Todd-Brown et al., 2013). Elevation gradients, that include both climatic and vegetation changes (i.e., bioclimatic gradients; Körner, 2007), have been used as surrogate experimental systems to predict long-term responses of ecosystem processes to climate change. In these space-for-time substitutions, changes in ecosystem pools and fluxes along an elevational gradient are used to predict potential changes in these characteristics over decadal to centennial time scales, assuming a directional shift in temperature (Pickett, 1989). However, most studies evaluating the impacts of elevational gradients on nutrient pools have been conducted in relatively humid forests, where temperature is the primary driver of ecosystem change not water availability (e.g., subtropical humid forests and tropical rainforests; He et al., 2016; Moser et al., 2011; Phillips et al., 2019). Elevational gradient impacts on nutrient pools in seasonally dry forests have been overlooked.

We synthesized ecosystem productivity and nutrient composition in vegetation and the entire regolith (soil + saprock) along a 2300 m elevational gradient in the southern Sierra Nevada, California (Barnes, 2020; Kelly, 2014; Moreland, 2020; Tian et al., 2019). Specifically, we addressed the following questions: 1) How do ecosystem productivity, litterfall nutrient fluxes, and nutrient stocks in vegetation, soil, and saprock vary with elevation?; 2) How do climate (i.e., temperature and precipitation) and regolith properties (e.g., stocks of N and P) influence the C stock in vegetation and regolith along the elevational gradient?; 3) To what degree are estimated MRTs of ecosystem C underestimated if based on C stock contained within surficial soil as opposed to the entire regolith?; and 4) How do estimated MRTs of ecosystem C based on the entire regolith change along an elevational gradient and following a major drought event? Answers to these research questions will improve our understanding of how climate change impacts ecosystem structure and function in Mediterranean-climate regions, some of the most vulnerable to climate warming.

2 Methods

2.1 Site Description

The Southern Sierra Critical Zone Observatory (SSCZO) bioclimatic gradient is located on the western slope of southern Sierra Nevada in California, spanning from 405 to 2700 m in elevation (Figure 1). The lowest site is an oak savannah at 405 m elevation within the San Joaquin Experimental Range (37°6.484' N, 119°43.949' W). Soils at this site are classified primarily as members of the Ahwahnee (coarse-loamy, mixed, active, thermic Mollic Haploxeralfs) and Vista (coarse-loamy, mixed, superactive, thermic Typic Haploxerepts; Beaudette & O'Geen, 2016) soil series. Dominant overstory vegetation includes blue oak (*Quercus douglasii* Hook. & Arn.) and interior live oak (*Quercus wislizeni* A. DC.), with an understory of evergreen shrubs and naturalized, exotic annual grasses. Going up in elevation, the next site is a pine-oak forest at 1160 m at Soaproot Saddle (37°2.4' N, 119°15.42' W). The main soil series at this site are Holland (fine-loamy, mixed, semiactive, mesic Ultic Haploxeralfs) and Chaix (coarse-loamy, mixed, superactive, mesic Typic Dystroxerepts). Dominant overstory vegetation includes ponderosa pine (*Pinus ponderosa* Douglas ex C. Lawson), incense cedar (*Calocedrus decurrens* (Torr.) Florin), canyon live oak (*Quercus chrysolepis* Liebm.), and a dense understory of evergreen and deciduous shrubs. The third site is a mixed-conifer forest at 2015 m elevation near Providence Creek (37°3.120' N, 119°12.196' W). Major soil series at this site include Gerle (coarse-loamy, mixed, superactive, frigid Humic Dystroxerepts) and Cagwin (mixed, frigid Dystric Xeropsamments; Bales et al., 2011). Dominant overstory vegetation includes ponderosa pine, Jeffrey pine (*Pinus jeffreyi* Balf.), white fir (*Abies concolor* (Gordon) Lindley ex Hildebrand), sugar pine (*Pinus lambertiana* Douglas), and incense cedar, with a patchy understory of evergreen and deciduous shrubs. The fourth, and highest elevation site is a subalpine forest at 2700 m elevation near Short Hair Creek (37°4.049' N, 118°59.204' W). Soils at this site are classified as members of the Stecum series (sandy-skeletal, mixed Typic Cryorthents; Gillespie & Zehfuss, 2004). Dominant overstory vegetation includes lodgepole pine (*Pinus*

contorta Loudon ssp. *Murrayana* (Grev. & Balf.) Critchf.) and red fir (*Abies magnifica* A. Murray bis), with a patchy understory of perennial herbs.

Mean annual air temperature (MAAT) and mean annual precipitation (MAP) are (respectively) 16.7 °C and 481 mm y^{-1} in the oak savannah, 14.0 °C and 815 mm y^{-1} in the pine-oak forest, 9.4 °C and 1018 mm y^{-1} in the mixed-conifer forest, and 4.8 °C and 1139 mm y^{-1} in the subalpine forest (period of record 1970 – 2020; 800-m resolution PRISM; https://www.prism.oregonstate.edu/). From 2012 to 2016, California experienced a historic multi-year drought, with near-record low precipitation combined with above-average temperatures (Diaz & Wahl, 2015; Robeson, 2015). This major drought event contributed to relative losses of tree basal area between 2010 and 2016 of 2% in the oak savannah, 79% in the pine-oak forest, 21% in the mixed-conifer forest, and 6% in the subalpine forest (Bales et al., 2018; Goulden & Bales, 2019). More detailed site characteristics have been described previously (Hunsaker et al., 2012; Johnson et al., 2011; O'Geen et al., 2018) and can also be found at the SSCZO website (http://criticalzone.org/sierra/infrastructure/field-areas-sierra/). The SSCZO program was decommissioned in year 2020. Future meteorological and biogeochemical datasets can be found at the nearby National Ecological Observatory Network sites with similar environmental conditions (https://www.neonscience.org/field-sites).

2.2 Ecosystem Productivity

The net ecosystem exchange of carbon dioxide (NEE) was measured every half hour since October 2009, using one eddy covariance flux tower situated at each of the four sites (https://www.ess.uci.edu/~california/). Ecosystem respiration rate (ER) was determined as the y-intercept of a linear fit to the half-hour NEEs during turbulent periods with incoming solar radiation less than 200 W m^{-2}. The half-hour gross ecosystem exchange (GEE) was calculated as the difference between observed NEE and ER. Gross primary productivity (GPP, Mg C ha^{-1} y^{-1}) and net ecosystem productivity (NEP, Mg C ha^{-1} y^{-1}) were the annual cumulative GEE and NEE, respectively (Goulden et al. 2012; Kelly 2014). We reported the pre-drought GPP, NEP, and ER by averaging annual values in water years (WY)

2010 – 2012. Post-drought GPP were the average annual values of WY 2015 and 2016, and were used for estimating the MRT of ecosystem C following the drought period.

2.3 Litterfall Nutrient Concentrations and Fluxes

Litterfall samples were collected using forty litter traps equally spaced on a grid within the same one ha plot at each site (Kelly, 2014). Litter traps were emptied two times each year: in autumn after most of the litterfall had occurred and in the following summer before the next litterfall season. Litter collection was conducted across multiple years at each site: WY 2010 – 2011 in oak savannah, WY 2011 – 2013 in the pine-oak and subalpine forests, and WY 2010 – 2013 in the mixed-conifer forest. The trap size was 0.74 m × 0.74 m across all sites and years, except for WY 2012 – 2013 in the mixed-conifer forest, where a new size of litter traps (0.28 m × 0.56 m) was used because the former traps were destroyed by heavy snowfall.

Litterfall samples from each trap were sorted to remove woody materials greater than 1-cm diameter and non-litterfall contaminants (e.g., dead insects), oven-dried at 65 – 70 °C for 72 h, and weighed. Sample measurements in WY 2012 were not included because collections only occurred in autumn at all four sites. Because litterfall nutrient concentrations are often less variable than litterfall mass across years (Yang et al., 2017), we analyzed nutrient concentrations on annual composites by trap for the forty samples collected only in one year (WY 2010 for the mixed-conifer forest and WY 2011 for the oak savannah, pine-oak forest, and subalpine forest). Concentrations of N and P were measured using Kjeldahl digestion followed by diluted digestate analysis with a Lachat AE Flow Injection Auto Analyzer (Method 13-107-06-2-D for N and Method 13-115-01-1-B for P, Lachat Instruments, Inc., Milwaukee, WI, USA). The site-level concentrations for litterfall N and P (%) were calculated using the average concentration of the forty composited samples at each site. Litterfall C concentrations were not measured and assumed to be 50% for all species for flux calculations (Guo et al., 2013; Neumann et al., 2018). We multiplied the mean nutrient concentration of forty samples measured in WY2010 or WY 2011 by the mean weight of sample annual-composites taken from each of the 40 traps per site measured across

different years to calculate the nutrient fluxes (kg ha^{-1} y^{-1}) at each site in each year. Mean annual litterfall nutrient fluxes were the average nutrient fluxes across different years. Our estimates did not include grass productivity, which can be an important pathway of nutrients into soils in oak savannah. Mean annual grass nutrient fluxes in the oak savannah site were estimated at 335 kg ha^{-1} y^{-1} for C, 3.6 kg ha^{-1} y^{-1} for N, and 0.9 kg ha^{-1} y^{-1} for P, based on measured annual grass productivity (WY 2010 – 2013; Becchetti et al., 2016) and nutrient concentrations within the San Joaquin Experimental Range, California (46% for C measured in summer, Barnes, 2020; 0.5% for N and 0.13% for P measured immediately following senescence, Woodmansee & Duncan, 1980).

2.4 Vegetation Nutrient Concentrations and Stocks

The diameter at breast height (DBH, 1.4 m) of all live trees > 0.10 m were measured within a one-ha plot oriented around the flux tower at each site during the 2009 and 2010 growing seasons (Kelly, 2014). Total aboveground biomass (AGB) was estimated based on the DBH and species-specific allometric equations (Matchett et al., 2015). Biomass of foliage, branches, stem bark, stem wood, coarse roots (> 2 mm diameter), and fine roots (< 2 mm diameter) were estimated based on their proportions to AGB by species (Jenkins et al., 2003 for aboveground components and Chojnacky et al., 2014 for coarse and fine roots).

We collected green leaves from 6 – 12 individuals (i.e., field replicates) of the eight dominant overstory species within the same one-ha plot across the four sites in August 2018 and 2019 (Figure S1 in Supporting Information S1). Green leaves were collected from the outer, sunlit portion of the upper third crown of each individual and composited for nutrient concentration measurements. We used the same analytical methods for green leaves to measure N and P concentrations as with litterfall samples, except we measured C concentrations in green leaves using dry combustion on an elemental analyzer (Costech Analytical ECS 4010 Elemental Analyzer, Costech Analytical Technologies, Inc., Valencia, CA). Green leaves were not collected for incense cedar, sugar pine, white fir, and red fir. Therefore, we used the average foliar C concentration (53.5%) of measured conifer species at our sites to estimate the four

unmeasured species because of the small variations in foliar C concentrations among those measured species (coefficient of variation was 3% among foothill pine, Jeffery pine, ponderosa pine, and lodgepole pine; Figure S1 in Supporting Information S1). Variations in foliar N and P concentrations among those measured conifer species were relatively large (i.e., 15% and 19%, respectively); hence, we used foliar N and P concentrations reported from the literature for the unmeasured species (Figure S1 in Supporting Information S1). To estimate the site-level nutrient concentration in green leaves (%), we averaged values from all overstory species weighted by the proportion of foliar biomass represented by each species to the total amount of foliar biomass in that one-ha plot at each site. We did not measure nutrient concentrations in aboveground woody tissues or roots. We considered C concentrations to be 50% in all non-foliar components of all tree species (Fahey et al., 2005), and used N and P concentrations from the literature to estimate nutrient stock in these tree tissues (Table S1 in Supporting Information S2). Site-level overstory nutrient stock (Mg ha^{-1}) was calculated as the sum of whole-tree nutrient stocks in all trees within the one-ha plot.

We did not measure the biomass of understory vegetation (mainly shrubs and herbaceous plants). To evaluate the contribution of understory vegetation to ecosystem nutrient storage, we used modeled biomass of shrubs and herbaceous plants at low-, mid-, and high-elevations in the same year of overstory inventory (2009) from a dynamic global vegetation model (i.e., Lund-Potsdam-Jena General Ecosystem Simulator; Guo et al., 2022). Nutrient stocks were estimated to be smaller in understory than overstory vegetation across all sites; the proportion of understory nutrient stocks to overstory nutrient stocks decreased from oak savannah (15%, 55%, and 78% for C, N, and P, respectively) to pine-oak and mixed-conifer forest (2%, 20%, and 12%) and then to subalpine forest (< 1%, 6%, and 3%), based on the modeled biomass and understory nutrient concentrations in the literature (Table S2 in Supporting Information S2). Nutrient stocks including both overstory and understory were lowest in low elevation, oak savannah and highest in high elevation, subalpine forest (Table S2 in Supporting Information S2), which was similar to the elevational trends in nutrient stocks of overstory alone. Thus, excluding

understory biomass and nutrient stock does not bias our interpretations of changes in ecosystem nutrient storage under warming using a space-for-time substitution.

2.5 Regolith Nutrient Concentrations and Stocks

Four soil pits were excavated within the same one-ha plot at each site in 2015 and 2016. The locations of four soil pits were determined to be representative of the major topographic features of the landscape at each site. We sampled the entire regolith profile by genetic horizons to a depth of hard bedrock, including soil (the O, A, and B) and saprock horizons in oak savannah and the subalpine forest, with average depths of the four pits of 164 cm and 100 cm, respectively. We did not acquire the entire saprock horizon at the two mid-elevation sites, with average depths of four pits of 222 cm in the pine-oak forest and 164 cm in the mixed-conifer forest (Figure S2 in Supporting Information S1). Therefore, we collected five Geoprobe samples until refusal with average depths of 424 cm and 950 cm, respectively.

Bulk density was calculated as the weight of the oven-dried fine fraction (< 2 mm dia.) divided by the volume of the oven-dried fine fraction (< 2 mm). The volume percent of gravel (> 2 mm) in soil and saprock was estimated by dividing the weight of the coarse fraction by 2.65 Mg m^{-3}, and then dividing this value by the total volume of fine and coarse fractions (Barnes, 2020). Soil pH was measured on air-dried and sieved materials in 0.01 M $CaCl_2$ with a 1:2 (5 g:10 ml) mixture (Thomas & Sparks, 1996). Particle size analysis was conducted on oven-dried and sieved materials using the hydrometer method (Gee & Bauder, 1986). We conducted these measurements for soil and saprock from soil pits and for Geoprobe samples taken below the average lower boundary of soil pits at the two mid-elevation sites. We reported % clay, % silt, and pH_{CaCl_2} by averaging three horizons (A, B, and saprock) across four pits, weighted by bulk density, thickness, and rock fraction.

We measured nutrient concentrations in all horizons from soil pits and Geoprobe samples. Concentrations of organic C and total N were determined using dry combustion on an elemental analyzer (Costech Analytical ECS 4010 Elemental Analyzer, Costech Analytical Technologies, Inc., Valencia, CA). Total P concentrations were determined by lithium metaborate fusion (Lajtha et al., 1999), and

measured with an inductively coupled plasma-optical emission spectrometer (Perkin-Elmer Optima 5300 DV, Environmental Analytical Laboratory at University of California, Merced). For the mid-elevation sites where soil and saprock samples from both pits and Geoprobe samples were taken, nutrient concentrations in the saprock were estimated based on the weighted average value of soil pits and Geoprobe samples, and the standard deviation of the total was propagated for addition (for details, see Barnes, 2020). Stocks of C, N, and P in each horizon (kg m^{-2}) were calculated using measured concentrations (%) multiplied by the thickness (m) of the sampled layer and the measured bulk density (Mg m^{-3}), and then multiplied by 1– rock fraction (vol%). We reported the site-level nutrient stock for each horizon and the entire regolith profile (Mg ha^{-1}) using the average values from the four soil pits at each site.

2.6 Data Analyses on Ecosystem Productivity and Nutrient Fluxes and Stocks

Elevational changes in ecosystem productivity and nutrient fluxes and stocks were examined by fitting linear and quadratic regression models in proc mixed using SAS 9.4 (SAS Institute, Inc. 2013). The dependent variables were: pre-drought GPP; pre-drought NEP; pre-drought ER; litterfall fluxes of C, N, and P; and stocks of C, N, and P in overstory vegetation, each master horizon (i.e., O, A, B, and saprock), and the entire regolith profile. We used elevation as the independent variable for linear regressions, and elevation and elevation^2 as the two independent variables for quadratic regressions. In each case, we chose the model with the lowest AICc (the Akaike information criterion that corrects for small sample sizes, AICc). A simpler model (i.e., linear) was chosen if two models had similar AICc values (differing by < 2; Burnham & Anderson, 2002). Additionally, we applied one-way ANOVAs with Tukey's Honest Significant Difference (HSD) tests to identify differences in the above dependent variables among the four sites; tests were not conducted for overstory nutrient stocks because values were estimated for the whole one-ha plot at each site. We applied the same analyses to nutrient concentrations in overstory green leaves, litterfall, and each regolith master horizon to help understand the elevational changes in nutrient fluxes and stocks (Figure S3 in Supporting Information S1). For the above analyses,

data were log-transformed to meet the assumption of normality and homoscedasticity of the residuals. A priori alpha level of 0.10 was used to evaluate statistical significance because of the greater variation typically found in field studies (Amrhein et al., 2019).

Structural equation modeling (SEM) was used to investigate the influences of potential environmental factors on regolith C stock. This analysis uses a multivariate statistical framework to examine linear causal relationships among variables. It allows us to examine both direct and indirect associations between C stock and influencing factors, as well as evaluate the relative importance of each factor (informed by the standardized regression coefficients; Gustafsson & Martenson, 2002). Environmental factors were MAAT, MAP, and regolith properties known to constrain uptake of water and nutrients, and hence vegetation productivity, including % clay, % silt, pH_{CaCl_2}, N stock, and P stock. We included values from individual pits in the model to increase the power of the analysis, assuming four pits at a minimum horizontal distance of 50 m apart were independent within each site. We examined the direct impact of climate (i.e., MAAT and MAP) and regolith properties (i.e., weighted mean % clay, % silt, and pH_{CaCl_2} for mineral soils and saprock, and total regolith N and P stocks) on total regolith C stock (n = 16). The indirect impact of climate on total regolith C stock was evaluated by examining its influences on regolith properties. We also performed the same analyses for C stock in the A, B, and saprock horizons individually (n = 16) to examine if the influences of climate and regolith properties on regolith C stock would vary by depth. We did not perform the analysis for C stocks in the O horizons because this horizon, by definition, does not have a soil texture and we did not make pH_{CaCl_2} measurements on this horizon. The SEM was conducted on log-transformed values using the maximum likelihood method in Amos software (version 21, Chicago, IL, USA). We were not able to apply the SEM for overstory C stock and productivity data because of the small number of statistical replicates (n = 4 because our measurement unit was the whole one-ha plot at each site). Instead, we examined the relationship among climate (i.e., MAAT and MAP), regolith properties (i.e., weighted mean % clay, % silt, and pH_{CaCl_2} for the mineral soil and saprock horizons, and total regolith stocks of C, N and P), and

vegetation (i.e., overstory C stock, GPP, NEP, ER, and litterfall C flux) using a Pearson correlation test based on the log-transformed datasets in SAS.

2.7 Data Analyses on Mean Residence Times of Ecosystem C

The MRTs of ecosystem C can be estimated as the ratio of total ecosystem C pools to GPP, assuming that the ecosystem is neither gaining nor losing C (i.e., steady-state conditions; Carvalhais et al., 2014). We could have also used the total output flux of C (i.e., ER) instead of GPP to calculate the MRTs because of the steady-state assumption. However, estimates of ER are less reliable than GPP estimates using eddy covariance due to the challenges in measuring nighttime gaseous fluxes in mountainous terrain (Goulden et al., 1996); in contrast, measurements of daytime fluxes (i.e., GEE) are comparatively reliable in both mountainous and flat terrain (Turnipseed et al., 2002, 2003).

We estimated the pre-drought MRT using the sum of overstory and regolith C stocks divided by the pre-drought GPP at each site. We evaluated the importance of including C stock in deep soil and saprock in our estimates by comparing the MRTs calculated using different ecosystem C stock values divided by the same pre-drought GPP. Different ecosystem C stock values included: overstory shoot and root biomass; overstory plus O horizon; overstory plus O and A horizons; overstory plus O, A, and B horizons; and overstory plus O, A, B, and saprock horizons. We used one-time measurements of C stock and multi-year measurements of GPP for the MRT estimates because C stock has a much smaller interannual variation than C input and output fluxes at an ecosystem scale. Note that, our estimates of MRTs assume that soil and saprock respond to a changing climate as a single C pool. However, C in soil and saprock that is stabilized by chemical or physical processes usually respond to warming at different rates (Li et al., 2020; Moreland et al., 2021; Song et al., 2012).

We used a space-for-time substitution to project changes in overstory C stock, total regolith C stock, pre-drought GPP, and corresponding MRTs, with increases in MAAT. In this approach, change in ecosystem structure and function that will occur in the future with a given increase in MAAT is estimated from these same characteristics found currently in another ecosystem at a lower elevation (and hence with

a higher MAAT). This approach relies on the assumption that factors driving spatial and temporal variations in ecosystem processes are the same, and ecosystems have reached steady-state conditions in their new climate (Pickett, 1989). This approach is suitable for studying warming impacts on vegetation C stock in the Sierra Nevada and other montane regions because vegetation change associated with warmer temperatures is relatively unimpeded by plant propagule dispersal (Kelly & Goulden, 2008; Rumpf et al., 2018; Steinbauer et al., 2018). The space-for-time substitution is also the only field-based experiment to help describe soil changes over multimillennial time scales (Richter et al., 2007), and has been used previously to assess long-term climate-driven changes in soil C stock (Adhikari et al., 2019; Ziegler et al., 2017). We projected overstory and total regolith C stock and pre-drought GPP based on their relationships with elevation (Figure S4 in Supporting Information S1), but not directly with MAT, to account for other environmental factors that covary under rising air temperatures (i.e., MAP, vegetation type, soil properties). For example, upward vegetation migrations are often accelerated at lower elevations with more frequent disturbances (Guo et al., 2018), but delayed at higher elevations due to constraints of shallower and nutrient-poorer soils on root development (Hagedorn et al., 2019; Maxwell et al., 2018). We estimated the local temperature lapse rate to be 5.2 °C per km based on the linear relationship between the MAAT and elevation ([MAAT, °C] = -5.20 × [Elevation, km] + 19.38, $p < 0.01$, $R^2 = 0.98$, n = 4; Figure S4 in Supporting Information S1), similar to the average environmental lapse rate in the lower atmosphere (6.5 °C per km, Barry & Chorley, 1987). Thus, the forest C stock and GPP at 192 and 385 m elevation below each of our four sites can be considered as the potential values with an increase in the MAAT of 1.0 and 2.0 °C, respectively. We then calculated the MRTs based on those projected values, assuming steady-state. We estimated percent changes in the overstory C stocks, total regolith C stocks, pre-drought GPPs, and MRTs due to these projected increases in MAAT from the projected values minus the measured estimates in the current climate, and then dividing these quantities by the current estimates for each site.

To examine changes in MRT following a major drought event at each site, we first estimated the remaining live trees in years following the four-year drought condition (i.e., year 2016 and 2017) to

determine post-drought C stock in overstory vegetation. We applied the percent dead trees per ha documented in the Sierra (relative tree losses between year 2012 and year 2016 – 2017; DeSiervo et al., 2018; Fettig et al., 2019) to our pre-drought tree inventory (year 2009 and 2010) by species and DBH at each site (Figure S5 in Supporting Information S1). Percent dead trees were estimated to be 9% in oak savannah, 41% in the pine-oak forest, 32% in the mixed-conifer forest, and 14% in the subalpine forest (Figure S6 in Supporting Information S1 and Table S3 in Supporting Information S2). We used a Monte Carlo simulation (2,000 iterations) to randomly draw estimated remaining numbers of live trees by species and DBH size from our pre-drought inventory, and then used the same allometric equations and C concentrations mentioned above for calculating post-drought overstory C stock. The post-drought MRT was then estimated using the sum of total regolith C stock and projected post-drought overstory C stock, divided by the measured post-drought GPP at each site. We reported the percent changes in ecosystem C stock, GPP, and MRT using the difference between the post-drought and pre-drought estimates, divided by the latter for each site.

3 Results

3.1 Ecosystem Productivity and Nutrient Fluxes and Stocks Along the SSCZO Bioclimatic Gradient

Pre-drought GPP and NEP showed similar trends across the bioclimatic gradient, with values highest at two mid-elevation sites (mixed-conifer and pine-oak forests). Specifically, pre-drought GPP and NEP increased from the subalpine forest (4.8 ± 0.4 and 2.6 ± 0.4 Mg C ha^{-1} y^{-1}, respectively, mean and standard error of three WY) to the mixed-conifer forest (12.5 ± 0.7 and 9.8 ± 0.5), and decreased from the pine-oak forest (16.8 ± 0.3 and 10.3 ± 0.6) to oak savannah (8.6 ± 0.8 and 0.2 ± 0.4; $R^2 = 0.99$, $p = 0.04$, n = 4, quadratic fitted with elevation for both; Figure 2). Pre-drought ER increased linearly with decreasing elevation ($R^2 = 0.98$, $p < 0.01$, n = 4; Figure 2).

Overstory C stocks were similar between the subalpine (155.8 Mg C ha^{-1}) and mixed-conifer forest (147.4), decreasing from the pine-oak forest (86.0) to the oak savannah (24.3; $R^2 = 0.99$, $p = 0.05$, n = 4, quadratic regression fitted with elevation; Figure 3a and 3c). Overstory stocks of N and P were again greater in the subalpine and mixed-conifer forest compared to the pine-oak forest and oak savannah (Figure 3d, 3f, 3g, and 3i). Annual litterfall fluxes of C, N, and P were greater in the pine-oak and mixed-conifer forests compared to oak savannah and the subalpine forest (based on ANOVA; Figure 3a, 3c, 3d, 3f, 3g, and 3i).

Total regolith C stock was greater in the pine-oak (222.2 ± 35.1 Mg ha^{-1}, mean and standard error of four replicated pits) and mixed-conifer forests (235.7 ± 16.5) compared to oak savannah (56.5 ± 5.7) and the subalpine forest (122.1 ± 20.3, based on ANOVA, $p < 0.01$; Figure 3b and 3c). Total regolith stocks of N and P peaked again at the two mid-elevation sites along the SSCZO bioclimatic gradient (based on ANOVA, $p \leq 0.02$; Figure 3e, 3f, 3h, and 3i). In O horizons, stocks of C, N, and P were statistically similar among the pine-oak, mixed-conifer, and subalpine forests; the oak savannah did not have an O horizon (based on ANOVA; Figure 3c, 3f, and 3i). In A horizons, stocks of C, N, and P were greater in the pine-oak forest compared to oak savannah, the mixed-conifer forest, and the subalpine forest ($p = 0.03$; Figure 3c, 3f, and 3i). In B horizons, elevational patterns of nutrient stocks varied across nutrient elements. Specifically, C stocks in B horizons were lower in oak savannah compared to the other three sites at higher elevations ($p = 0.02$; Figure 3c), whereas N stocks were similar among the four sites ($p = 0.46$; Figure 3f), and P stocks were lower in the subalpine forest than the other three sites at lower elevations ($p = 0.03$; Figure 3i). In saprock horizons, stocks of C, N, and P were greatest in the mixed-conifer forest among the four sites, where saprock was thickest ($p \leq 0.01$; Figure 3c, 3f, 3i).

3.2 Influences of Climate and Regolith Properties on C Stocks in Regolith and Vegetation

The SEM showed that both climate and regolith properties helped explain changes in regolith C stock along the SSCZO bioclimatic gradient. For total regolith C stock, the most direct influential factor was total regolith N stock, followed by MAP and MAAT (Figure 4a). Other tested factors had relatively

small influences on total regolith C stock, including % silt, % clay, pH_{CaCl2}, and total regolith P stock. Based on the standardized total impact, MAP was the most influential factor among all factors tested (Figure 4b). In each master horizon, the strength of influence of individual predictive factors of regolith C stock were different among horizons. For example, climate (i.e., MAP and MAAT) had direct impact on C stock in B and saprock horizons but not in A horizons, and P stock had a direct impact on C stock in A horizons but not in B and saprock horizons (Figure 4c, 4e, and 4g). Based on the standardized total impact, MAP was the most influential factor on the size of the soil C stock among all factors evaluated in A and B horizons; in saprock horizons, N stock exerted the most influence on the size of the C stock (Figure 4d, 4f, and 4h).

Influences of climate and regolith properties on overstory C stock and ecosystem productivity were not examined using the SEM because of the small number of statistical replicates. Pearson correlation tests among climate, regolith properties, and vegetation revealed that: MAP was positively correlated with overstory C stock along the SSCZO bioclimatic gradient ($p < 0.01$, $r = 0.99$, n = 4; Figure 5); GPP was positively correlated with total regolith P stock ($p = 0.05$, $r = 0.94$; Figure 5); and NEP was positively correlated with litterfall C flux ($p = 0.06$, $r = 0.94$), % silt ($p < 0.01$, $r = 0.99$), and total regolith C stock ($p < 0.01$, $r = 0.99$) along the bioclimatic gradient.

3.3 Mean Residence Times of Ecosystem C and Response to Projected Rising Air Temperatures and a Major Drought

The MRT of ecosystem C was longer at higher compared to lower elevation sites (based on MRT estimates using the sum of overstory and total regolith C stock divided by the pre-drought GPP). Along the SSCZO bioclimatic gradient, MRT of ecosystem C was 10 y in oak savannah, 18 y in pine-oak forest, 31 y in mixed-conifer forest, and 57 y in subalpine forest (Figure 6). The MRTs would be substantially underestimated at each site if the calculation was based on an incomplete accounting for the size of the total regolith C stock. For example, estimated MRT based on C stock in overstory plus O and A horizons, decreased by 4 y (39%) in oak savannah, 6 y (32%) in pine-oak forest, 14 y (45%) in mixed-conifer

forest, and 14 y (24%) in subalpine forest compared to estimates based on C stock in overstory plus whole-regolith profile (O+A+B+saprock horizons; Figure 6).

The MRTs of ecosystem C decreased with projected increases in MAAT (Figure 7). This result is based on statistical regressions among overstory C stock, total regolith C stock, pre-drought GPP, and the current MAAT along the SSCZO bioclimatic gradient. With an increase of 2.0 ℃ in MAAT, the projected MRTs of ecosystem C decreased by 3 y (27%) in oak savannah, 4 y (25%) in pine-oak forest, 7 y (24%) in mixed-conifer forest, and 19 y (30%) in subalpine forest compared to the estimates under the current climate. However, projected changes in overstory and total regolith C stocks and pre-drought GPP varied among the four elevation sites. Overstory C stock decreased in oak savannah, pine-oak, and mixed-conifer forests, but slightly increased in subalpine forest with increasing MAAT (Figure 7). Total regolith C stock and pre-drought GPP decreased in oak savannah and pine-oak forest (Figure 7a and 7b), but increased in mixed-conifer and subalpine forests with increasing MAAT (Figure 7c and 7d).

A major drought event increased the MRTs of ecosystem C along the SSCZO bioclimatic gradient. Post-drought MRTs were estimated using the sum of measured total regolith C stock and projected post-drought overstory C stock, divided by the post-drought GPP. Following the four-year drought event and compared to the pre-drought MRTs, the estimated MRT increased most in pine-oak forest (by 35 y or 191% increase) and least in oak savannah by (1 y or 8% increase). Increases in the MRT were intermediate in mixed-conifer (9 y or 31% increase) and subalpine forests (21 y or 37% increase; Figure 8a). Percent reductions in overstory C stock and GPP following the drought event were also greatest in pine-oak forest compared to the other three sites (Figure 8).

4 Discussion

The Sierra Nevada of California is one of the major mountain ranges in western North America. It is also found within one of the five Mediterranean-climate regions worldwide that have dense human population and direct linkages to global food production (Rick et al., 2020). Hence, understanding C cycles in Sierran forests is important to model projections of regional and global C storage. We

investigated nutrient pools along a 2300-m bioclimatic gradient on the western slope of this mountain range and used a space-for-time substitution to examine vegetation and regolith C stocks in association with MAAT, MAP, and regolith properties (i.e., %clay, %silt, pH_{CaCl2}, N stock, and P stock). We estimated the mean residence time of ecosystem C and projected its changes with rising mean annual air temperatures (space-for-time substitution) and following a major drought, assuming steady state conditions. This study advances the knowledge of C storage in the critical zone and forest ecosystems facing a warmer and drier climate.

4.1 Vegetation and Soil Nutrient Storage to Climate Warming

Lower overstory C stock with decreasing elevation (Figure 3a) suggests that warmer conditions will reduce vegetation biomass input and consequently C storage in the Sierra Nevada. In other seasonally dry forests, lower vegetation C stock has also been observed with decreasing elevation (e.g., Arizona's Coconino National Forest, Conant et al., 1998; China's Loess Plateau, Liu & Nan, 2018; California's northern Sierra Nevada, Mattson & Zhang, 2019). In contrast, increases in vegetation biomass and C stock with decreasing elevation has been observed along six elevational gradients (Moser et al., 2011) and temperature gradients in tropical rainforests (Raich et al., 2006). Thus, unlike humid forests where vegetation C storage has been found to increase with warmer temperatures and longer growing seasons, our findings demonstrate vegetation C storage in seasonally dry forests will decrease with warming because of enhanced water limitation; tree biomass in seasonally dry forests is strongly constrained by precipitation and water availability (e.g., Figure 5). In the Sierra Nevada, lower overstory biomass with decreasing elevation can also be attributed to reduced proportion of large trees (Figure S5 in Supporting Information S1), which may be due, in part, to the greater occurrence of disturbances below the subalpine zone (e.g., timber harvest, drought, and wildfire; Laudenslayer & Darr, 1990; Paz-Kagan et al., 2017; Schwartz et al., 2015). Climate is not commonly the primary control over vegetation C storage in humid forests. For instance, vegetation C stock decreased (e.g., the Brazilian coastal Atlantic Forests; Alves et

al., 2010; Vieira et al., 2011) or remained similar (e.g., the Hawaiian tropical wet forests; Selmants et al., 2014; the Ecuadorian tropical rainforests; Unger et al., 2012) with decreasing elevation in some humid forests, which was attributed to variations in topography and nutrient supply. Overall, changes in vegetation C storage with long-term warming are likely different between seasonally dry and humid forests, with some exceptions due to unique local conditions.

Regolith thickness plays a major role in determining nutrient storage in the regolith. We observed total regolith stocks of C, N, and P peaked at mid elevations along the SSCZO bioclimatic gradient primarily due to thicker saprock. Along the western slopes of the Sierra Nevada, mid-elevation forest ecosystems experience relatively high precipitation and mild temperatures. This favorable climate stimulates biological and mineral weathering processes, resulting in thick saprock at the pine-oak and mixed-conifer forest sites (Hasenmueller et al., 2017; Holbrook et al., 2014; Kelly & Goulden, 2016; Moreland et al., 2021; Tian et al., 2019). Regolith development is constrained by moisture conditions at the oak savannah (lower elevation) and by low temperatures and past glaciation at the subalpine forest sites (higher elevation; O'Geen et al., 2018). In the Sierra Nevada, regolith nutrient storage is also influenced by climate indirectly. For example, the mixed-conifer forest had thinner topsoil (thus smaller nutrient stocks) than the pine-oak forest (Figure 3b, 3e, and 3h) partially because of higher rates of surficial soil erosion with greater precipitation (Stacy et al., 2015; Yang et al., 2022), although they both receive a favorable climate for regolith development. Dust deposition of P to soils is substantial at our four sites, and can outpace the bedrock P input during drought years (Aarons et al., 2019; Aciego et al. 2017; Arvin et al., 2017). In montane forests experiencing a Mediterranean-type climate, nutrient storage in the regolith is strongly determined by regolith development and external processes that are sensitive to climate.

The unimodal response in C, N, and P stocks in the entire regolith with decreasing elevation suggests changes in regolith nutrient storage with long-term warming are elevation dependent. This unimodal pattern can be attributed to the inconsistent changes in nutrient input and output rates along the bioclimatic gradient, which is revealed by the nonlinear patterns of nutrient concentrations in soil and

saprock (Figure S3 in Supporting Information S1). In the Sierra Nevada, nutrient input rates peak at pine-oak and mixed-conifer forests compared to oak savannah and subalpine forest (e.g., litterfall input for C, N, and P in Figure 3 and weathering input of P in Figure S7 in Supporting Information S1), and nutrient output rates generally increase with decreasing elevation (e.g., soil organic matter decomposition; Wang et al., 2000 and ER in Figure 2 in this study). Thus, warming within the subalpine forest zone will largely increase nutrient inputs to soils, driven by stimulated rates of organic matter decomposition and saprock weathering under rising temperatures and unchanged precipitation. However, warming below the mixed-conifer and pine-oak forests will constrain nutrient inputs to soils by strongly reduced precipitation and water availability, along with increases in nutrient output with warmer conditions. In contrast, in relatively humid forests, soil C and N concentrations and stocks generally decrease linearly with decreasing elevation, suggesting a consistent decrease in soil C and N storage with warming among elevations (e.g., Dieleman et al., 2013; He et al., 2016; Sun et al., 2019; Tashi et al., 2016; Tsozué et al., 2019). Responses of soil P storage to warming in humid forests will vary among elevations, as nonlinear changes in soil P concentrations have been observed along an elevational gradient and attributed to influences of geochemical weathering and leaching (e.g., He et al., 2016). Clearly, nutrient storage in soil and saprock responses of seasonally dry forests to climatic warming are more complex than in humid forests because of water availability constraints on ecosystem responses in addition to changes in temperature (Hart et al., 1992).

4.2 Climate-Soil-Plant Interactions

We observed positive correlations between total regolith P stock and GPP based on the four sites (Figure 5), suggesting that warming-induced changes in soil and saprock nutrients will influence plant growth and productivity. Soil nutrient availability strongly influenced leaf development and plant growth along bioclimatic gradients in previous studies (He et al., 2016; Santiago et al., 2004, 2005; Tan & Wang, 2016). At our sites, available P concentrations in soil and saprock increased from the subalpine forest to the mixed-conifer and pine-oak forests (Figure S7 in Supporting Information S1), driven apparently by

higher apatite content in parent materials and decreased depletion rates (Barnes, 2020; O'Geen et al., 2018). Thus, changes in available P in the regolith mirrored that of foliar P from the subalpine to pine-oak forest. This result suggests that, above the pine-oak forest, increases in soil nutrient availability with warming will be sufficient to keep up with increased vegetation demand. In contrast, P availability in soil and saprock decreased from our mid to low elevation sites (Figure S7 in Supporting Information S1), suggesting vegetation productivity below the pine-oak forest will be constrained by available nutrients in the regolith with warming. Taken together, warming in seasonally dry forests will cause an imbalance between nutrient demand by the vegetation and nutrient supply from the regolith at sites that are currently warm (e.g., transitional Pine-Oak Forests), but nutrient supply and demand will be more balanced in sites that are currently colder (e.g., subalpine forests).

Understanding the factors controlling regolith C stocks is important for estimating the capacity for C storage belowground, yet it is unclear whether the same factors will govern C storage in surficial and deep regolith pools. Based on the standardized total impact from the SEM (Figure 4d and 4f), we found MAP remained the most influential factor on C stock in soil A and B horizons, suggesting climatic controls on soil C storage can remain significant even in subsoil horizons. Similar elevational changes in soil C stock have been observed across different depths above 1 m or different subordinate mineral horizons in other seasonally dry forests (e.g., Castillo-Velásquez, 2017) and humid forests (e.g., Ma & Chang, 2019; Tashi et al., 2016). These observations suggest, in part, that deep soil C can be as sensitive as surficial soil C to warming. However, *in situ* manipulative experiments have shown similar (e.g., Hicks Pries et al., 2017), lower (e.g., Soong et al., 2021), and higher (e.g., Jia et al., 2019) temperature sensitivities of deep soil C compared to surficial soil C, suggesting that the vulnerability of deep soil C storage to warming varies by site and will be dependent on C availability to microbes (Pries et al., 2021). We further observed strong influences of MAAT and MAP on C stock in the saprock (Figure 4g), a regolith layer that has weathered bedrock and lower biological activity. This is likely due to the strong regulation of climate on transport rates of dissolved organic matter from upper soil horizons (Marin-Spiotta et al., 2011; Rumpel & Kögel-Knabner, 2011) and saprock thickness available for C storage

(Moreland et al., 2021). The SEM also revealed that the C and N cycles will remain coupled within the entire regolith with climate warming (Figure 4). However, warming-induced changes in the influence of P cycle on C storage may only occur in surficial soils (Figure 4). To conclude, warming impacts on regolith C storage can remain substantial from the surficial to the bottom of the regolith profile layers.

4.3 Ecosystem C Persistence Under Warmer and Drier Conditions

Reductions in the MRTs of ecosystem C with projected warming were driven by different mechanisms among elevations. Below the mixed-conifer zone in the Sierra Nevada, the reduced MRTs of C with projected increases in MAAT were mainly driven by reductions in C stocks in overstory trees and regolith (Figure 7a, 7b). This result suggests that forest C stock at relatively warm sites will decrease with long-term warming due to reduced ecosystem productivity and increased plant and soil microbial respiration rates. From the mixed-conifer to subalpine zone, reduced MRTs with projected increases in MAAT were driven by large increases in GPP accompanied by decreases (mixed-conifer, Figure 7c) or comparatively smaller increases (subalpine, Figure 7d) in C storage within the overstory trees plus regolith pools. Thus, although long-term warming can increase forest C stock at relatively cold sites by increasing rates of ecosystem productivity and regolith forming processes, warming will also stimulate ecosystem respiration (as shown in Figure 2), partially offsetting ecosystem C gains (Melillo et al., 2011; Raich et al., 2006; Schlesinger & Andrews, 2000). In other forests experiencing a similar Mediterranean-type climate, an ecosystem process model (i.e., Biome-BGC) predicted slower rates of increase in forest C stock than GPP under a future climate scenario consisting of +2 °C and + 550 ppm CO_2 concentrations above the preindustrial level (Chiesi et al., 2010). Thus, changes in forest C storage may lag behind the rates of rising temperatures due, in part, to stimulated ecosystem respiration. Overall, long-term warming will reduce forest C persistence in Mediterranean-climate regions primarily by limiting primary productivity at warmer sites and increasing ecosystem respiration at colder sites.

Drought impacts on forest C persistence are largely unknown (van der Molen et al., 2011). However, understanding drought impacts on ecosystem C storage and accumulation is critical for

predictive model development because more frequent and severe drought events are predicted with climate warming (Brando et al., 2019; Williams et al., 2020). We observed increases in estimated MRTs of ecosystem C following a four-year drought event, driven by decreases in GPP to a greater degree than decreases in ecosystem C stock (Figure 8a). Although overstory trees at mid elevations can access water and nutrients from deep soil and saprock when the surface soils are relatively dry (Klos et al., 2018), higher mortality rates and greater reductions in overstory biomass following drought were observed at pine-oak and mixed-conifer forests compared to oak savannah and subalpine forests (Figure 8b). Hence, a multi-year drought event will pose severe threats to the vegetation at mid elevations in the Sierra Nevada by depleting the water reservoir in deep regolith (revealed by the lower water runoff relative to the near-average precipitation in the year following drought; Bales et al., 2018; Goulden & Bales, 2019). Relatively high drought-induced mortality rates at mid elevations can also be attributed to the species composition and tree density. For example, ponderosa pine and white fir that mostly occur at mid elevations are less resistant to drought compared to oak species at low elevation because of their poorer stomatal control and greater susceptibility to mortality from bark beetle infestation (Fettig et al., 2019; Garcia-Forner et al., 2017; Reed & Hood, 2021). Denser forests are more susceptible to drought-induced mortality because of the increased tree competition (Bradford & Bell, 2017). Drought-induced dead vegetation can exist and continue to release CO_2 at decadal and centennial time scales (Harmon et al., 2020; Woodall et al., 2021). With increased occurrence of major droughts under warmer conditions, more dramatic changes in forest C storage and persistence will occur at sites that originally receive a relatively favorable climate for ecosystem productivity.

5 Conclusions

Very few studies have reported the whole-ecosystem stocks of C, N, and P and their association with elevation and environmental factors in forests growing in Mediterranean climates. Using a space-for-time substitution along a bioclimatic gradient, our observations emphasize that warming-induced changes in nutrient storage and C persistence will differ in these seasonally dry forests compared to relatively

humid forests. Our findings have important implications for model projections of nutrient dynamics and C persistence under climate warming in seasonally dry forests. First, accurate descriptions of the current climate (e.g., MAAT and MAP) and predictions of future climate at the site level are important to help predict the complex changes in forest nutrient storage with warming. Second, our findings highlight the need to quantify and include nutrients in deep soil and weathered bedrock in model formulation as nutrients stored in deep regolith layers can be substantial and are responsive to a changing climate. Third, scenarios of warming-induced disturbances (e.g., a major drought) are needed in model predictions because these disturbances will strongly alter forest nutrient balance at decadal to centennial time scales. Because space-for-time substitution studies are observational and not experimental, the inferential power of the space-for-time substitution is limited. However, these observational studies are the only type of data-driven investigations currently available to forecast terrestrial ecosystem changes over time scales relevant to ecosystem development and long-term atmospheric changes. As such, the space-for-time substitution approach will be invaluable in the future to help constrain ecosystem and Earth system models to accurately project forest C storage in the context of climate change.

Data Availability Statement

All the data are available in the manuscript. Ecosystem productivity datasets are available at https://www.ess.uci.edu/~california/. Vegetation and regolith datasets have been archived on Figshare (overstory species and the diameter at breast height (DBH, 1.4 m), litterfall mass and concentrations, and nutrient stock, texture, and pH in soil and saprock, DOI: 10.6084/m9.figshare.21231794, https://doi.org/10.6084/m9.figshare.21231794; carbon concentrations in soil and saprock, DOI: 10.6084/m9.figshare.13106102, https://doi.org/10.6084/m9.figshare.13106102; bulk density of soil and saprock, DOI: 10.6084/m9.figshare.13106111, https://doi.org/10.6084/m9.figshare.13106111). Nitrogen and phosphorus concentrations in soil and saprock are accessible at Supplementary Table 2-S1 in Barnes, M. E. 2020. Climatic controls on critical zone nutrient biogeochemistry in Semiarid and Mediterranean

ecosystems (Doctoral dissertation). Retrieved from [eScholarship]. (https://escholarship.org/uc/item/1fr2r9h9) Location: University of California, Merced.

Acknowledgements

This study was primarily supported by grants from the National Science Foundation in support of the Southern Sierra Critical Zone Observatory (SSCZO; EAR-0725097, 1239521, and 1331939) and the Critical Zone Collaborative Network (Geomicrobiology and Biogeochemistry in the Critical Zone; EAR-2012878, 2012633, and 2012403). Additional funding sources included fellowships and grants from the Institute for the Study of Ecological Effects of Climate Impacts, University of California Graduate Division, Environmental System Graduate Group, Mildred E. Mathias Graduate Research Program. During the writing of this manuscript, Morgan Barnes was supported, in part, by the U.S. Department of Energy, Office of Biological and Environmental Research, Environmental System Science program through the River Corridor Scientific Focus Area project at the Pacific Northwest National Laboratory, and Kimber Moreland was supported, in part, by the Lawrence Livermore National Laboratory through UC Lab Fees Research Fellowship (LGF-18-488060). We specially thank Martha Conklin, Christina Tague, Clifford Riebe, Mohammad Safeeq, Liying Zhao, Xiande Meng, Ryan Bart, Nicholas Dove, Erin Stacy, Emma McCorkle, Weichao Guo, Guotao Cui, and other collaborators of the SSCZO for their contributions to our study. We thank the staff at the Sierra Nevada Research Institute and US Forest Service Pacific Southwest Research Station for their logistic support. We also thank past undergraduate researchers Oscar Elias, Madeline Castro, and Susan Glaser from UC Merced for their help in the field and laboratory in support of this project. Finally, we are grateful to two anonymous reviewers for their constructive comments to improve our manuscript.

Conflict of Interest

The authors declare no conflicts of interest for this study.

References

Aarons, S. M., Arvin, L. J., Aciego, S. M., Riebe, C. S., Johnson, K. R., Blakowski, M. A., et al. (2019). Competing droughts affect dust delivery to Sierra Nevada. *Aeolian Research*, **41**, 100545.

Aciego, S. M., Riebe, C. S., Hart, S. C., Blakowski, M. A., Carey, C. J., Aarons, S. M., et al. (2017). Dust outpaces bedrock in nutrient supply to montane forest ecosystems. *Nature Communications*, **8**(1), 1–10.

Adhikari, K., Owens, P. R., Libohova, Z., Miller, D. M., Wills, S. A., & Nemecek, J. (2019). Assessing soil organic carbon stock of Wisconsin, USA and its fate under future land use and climate change. *Science of the Total Environment*, **667**, 833–845.

Alexander, E. B. (2014). Foliar analyses of conifers on Serpentine and Gabbro soils in the Klamath Mountains. *Madroño*, **61**(1), 77–81.

Allen, K., Dupuy, J. M., Gei, M. G., Hulshof, C., Medvigy, D., Pizano, C., et al. (2017). Will seasonally dry tropical forests be sensitive or resistant to future changes in rainfall regimes?. *Environmental Research Letters*, **12**(2), 023001.

Alves, L. F., Vieira, S. A., Scaranello, M. A., Camargo, P. B., Santos, F. A., Joly, C. A., & Martinelli, L. A. (2010). Forest structure and live aboveground biomass variation along an elevational gradient of tropical Atlantic moist forest (Brazil*). Forest Ecology and Management*, **260**(5), 679–691.

Amrhein, V., Greenland, S., & McShane, B. (2019). Scientists rise up against statistical significance. *Nature*, **567**, 305–307.

Arvin, L. J., Riebe, C. S., Aciego, S. M., & Blakowski, M. A. (2017). Global patterns of dust and bedrock nutrient supply to montane ecosystems. *Science Advances*, **3**(12), eaao1588.

Bales, R. C., Hopmans, J. W., O'Geen, A. T., Meadows, M., Hartsough, P. C., Kirchner, P., et al. (2011). Soil moisture response to snowmelt and rainfall in a Sierra Nevada mixed-conifer forest. *Vadose Zone Journal*, **10**(3), 786–799.

Bales, R. C., Goulden, M. L., Hunsaker, C. T., Conklin, M. H., Hartsough, P. C., O'Geen, A. T., et al. (2018). Mechanisms controlling the impact of multi-year drought on mountain hydrology. *Scientific Reports*, **8**(1), 1-8.

Barnes, M. E. (2020). Climatic controls on critical zone nutrient biogeochemistry in Semiarid and Mediterranean ecosystems (Doctoral dissertation). Retrieved from [eScholarship]. (https://escholarship.org/uc/item/1fr2r9h9) Location: University of California, Merced.

Barry, R. G., & R. J. Chorley. (1987). Atmosphere, Weather, and Climate. 5th ed. Methuen, 460 pp.

Barrett, D. J. (2002). Steady state turnover time of carbon in the Australian terrestrial biosphere. *Global Biogeochemical Cycles*, **16**(4), 55.

Beaudette, D. E., & O'Geen, A. T. (2016). Topographic and geologic controls on soil variability in California's Sierra Nevada foothill region. *Soil Science Society of America Journal*, **80**(2), 341–354.

Becchetti, T. H. E. R. E. S. A., George, M. R., McDougald, N., Dudley, D., Connor, M., Flavel, D., et al. (2016). Annual range forage production. University of California Division of Agriculture and Natural Resources, Publication, 8018. https://anrcatalog.ucanr.edu/pdf/8018.pdf

Berner, L. T., Law, B. E., & Hudiburg, T. W. (2017). Water availability limits tree productivity, carbon stocks, and carbon residence time in mature forests across the western US. *Biogeosciences*, **14**(2), 365–378.

Boring, L. R., Swank, W. T., Waide, J. B., & Henderson, G. S. (1988). Sources, fates, and impacts of nitrogen inputs to terrestrial ecosystems: review and synthesis. *Biogeochemistry*, **6**(2), 119–159.

Bradford, J. B., & Bell, D. M. (2017). A window of opportunity for climate-change adaptation: easing tree mortality by reducing forest basal area. *Frontiers in Ecology and the Environment*, **15**(1), 11–17.

Brando, P. M., Paolucci, L., Ummenhofer, C. C., Ordway, E. M., Hartmann, H., Cattau, M. E., et al. (2019). Droughts, wildfires, and forest carbon cycling: A pantropical synthesis. *Annual Review of Earth and Planetary Sciences*, **47**, 555–581.

Burnham, K. P., & Anderson, D. R. (2002). A practical information-theoretic approach. Model selection and multimodel inference, 2nd ed. Springer, New York.

Campo, J. (2016). Shift from ecosystem P to N limitation at precipitation gradient in tropical dry forests at Yucatan, Mexico. *Environmental Research Letters*, **11**(9), 095006.

Carvalhais, N., Forkel, M., Khomik, M., Bellarby, J., Jung, M., Migliavacca, M., et al. (2014). Global covariation of carbon turnover times with climate in terrestrial ecosystems. *Nature*, **514**(7521), 213–217.

Castillo-Velásquez, K. D. (2017). Soil carbon stocks on a tropical forest altitudinal gradient are correlated with bioclimatic factors, soil properties and vegetation functional properties. (Master thesis). Retrieved from

[Dspace Home]. (http://201.207.189.89/handle/11554/8632) Location: The Tropical Agricultural Research and Higher Education Center.

Chiesi, M., Moriondo, M., Maselli, F., Gardin, L., Fibbi, L., Bindi, M., & Running, S. W. (2010). Simulation of Mediterranean forest carbon pools under expected environmental scenarios. *Canadian Journal of Forest Research*, **40**(5), 850–860.

Chojnacky, D. C., Heath, L. S., & Jenkins, J. C. (2014). Updated generalized biomass equations for North American tree species. *Forestry*, **87**(1), 129–151.

Conant, R. T., Klopatek, J. M., Malin, R. C., & Klopatek, C. C. (1998). Carbon pools and fluxes along an environmental gradient in northern Arizona. *Biogeochemistry*, **43**(1), 43–61.

Deitch, M. J., Sapundjieff, M. J., & Feirer, S. T. (2017). Characterizing precipitation variability and trends in the world's Mediterranean-climate areas. *Water*, **9**(4), 259.

DeSiervo, M. H., Jules, E. S., Bost, D. S., De Stigter, E. L., & Butz, R. J. (2018). Patterns and drivers of recent tree mortality in diverse conifer forests of the Klamath Mountains, California. *Forest Science*, **64**(4), 371–382.

Diaz, H. F., & Wahl, E. R. (2015). Recent California water year precipitation deficits: A 440-year perspective. *Journal of Climate*, **28**(12), 4637–4652.

Dieleman, W. I., Venter, M., Ramachandra, A., Krockenberger, A. K., & Bird, M. I. (2013). Soil carbon stocks vary predictably with altitude in tropical forests: Implications for soil carbon storage. *Geoderma*, **204**, 59–67.

Diffenbaugh, N. S., Swain, D. L., & Touma, D. (2015). Anthropogenic warming has increased drought risk in California. *Proceedings of the National Academy of Sciences*, **112**(13), 3931–3936.

Dixon, R. K., Solomon, A. M., Brown, S., Houghton, R. A., Trexier, M. C., & Wisniewski, J. (1994). Carbon pools and flux of global forest ecosystems. *Science*, **263**(5144), 185–190.

Fahey, T. J., Siccama, T. G., Driscoll, C. T., Likens, G. E., Campbell, J., Johnson, C. E., et al. (2005). The biogeochemistry of carbon at Hubbard Brook. *Biogeochemistry*, **75**(1), 109–176.

Fenn, M. (1991). Increased site fertility and litter decomposition rate in high-pollution sites in the San Bernardino Mountains. *Forest Science*, **37**(4), 1163–1181.

Fettig, C. J., Mortenson, L. A., Bulaon, B. M., & Foulk, P. B. (2019). Tree mortality following drought in the central and southern Sierra Nevada, California, US. *Forest Ecology and Management*, **432**, 164–178.

Friedlingstein, P., Meinshausen, M., Arora, V. K., Jones, C. D., Anav, A., Liddicoat, S. K., & Knutti, R. (2014). Uncertainties in CMIP5 climate projections due to carbon cycle feedbacks. *Journal of Climate*, **27**(2), 511–526.

Friedlingstein, P., Jones, M. W., O'sullivan, M., Andrew, R. M., Hauck, J., Peters, G. P., et al. (2019). Global carbon budget 2019. *Earth System Science Data*, **11**(4), 1783–1838.

Garcia-Forner, N., Biel, C., Savé, R., & Martínez-Vilalta, J. (2017). Isohydric species are not necessarily more carbon limited than anisohydric species during drought. *Tree Physiology*, **37**(4), 441–455.

Gee, G. W., & Bauder, J. M. (1986) Particle-size analysis. In: Methods of Soil Analysis, Part 1, Physical and Mineralogical Methods. Agronomy Monogroph No. 9 (2nd edition), American Society of Agronomy, Madison, WI, pp 383–411.

Gillespie, A. R., & Zehfuss, P. H. (2004). Glaciations of the sierra Nevada, California, USA. *In Developments in quaternary sciences* (Vol. 2, pp. 51–62). Elsevier.

Giorgetta, M. A., Jungclaus, J., Reick, C. H., Legutke, S., Bader, J., Böttinger, M., et al. (2013). Climate and carbon cycle changes from 1850 to 2100 in MPI‐ESM simulations for the Coupled Model Intercomparison Project phase 5. *Journal of Advances in Modeling Earth Systems*, **5**(3), 572–597.

Giorgi, F. (2006). Climate change hot-spots. *Geophysical Research Letters*, **33**(8), L08707.

Goulden, M. L., Anderson, R. G., Bales, R. C., Kelly, A. E., Meadows, M., & Winston, G. C. (2012). Evapotranspiration along an elevation gradient in California's Sierra Nevada. *Journal of Geophysical Research: Biogeosciences*, **117**, G03028.

Goulden, M. L., Munger, J. W., Fan, S. M., Daube, B. C., & Wofsy, S. C. (1996). Measurements of carbon sequestration by long-term eddy covariance: Methods and a critical evaluation of accuracy. *Global Change Biology*, **2**(3), 169–182.

Goulden, M. L., & Bales, R. C. (2019). California forest die-off linked to multi-year deep soil drying in 2012–2015 drought. *Nature Geoscience*, **12**(8), 632–637.

Gower, S. T. (2003). Patterns and mechanisms of the forest carbon cycle. *Annual Review of Environment and Resources*, **28**(1), 169–204.

Graham, R., Rossi, A., & Hubbert, R. (2010). Rock to regolith conversion: producing hospitable substrates for terrestrial ecosystems. *GSA Today*, **20**, 4–9.

Gross, C. D., & Harrison, R. B. (2019). The case for digging deeper: soil organic carbon storage, dynamics, and controls in our changing world. *Soil Systems*, **3**(2), 28.

Gu, C., Wilson, S. G., & Margenot, A. J. (2020). Lithological and bioclimatic impacts on soil phosphatase activities in California temperate forests. *Soil Biology and Biochemistry*, **141**, 107633.

Guo, Z., Hu, H., Li, P., Li, N., & Fang, J. (2013). Spatio-temporal changes in biomass carbon sinks in China's forests from 1977 to 2008. *Science China Life Sciences*, **56**(7), 661–671.

Guo, F., Lenoir, J., & Bonebrake, T. C. (2018). Land-use change interacts with climate to determine elevational species redistribution. *Nature Communications*, **9**(1), 1–7.

Guo, W., Safeeq, M., Liu, H., Wu, X., Cui, G., Ma, Q., et al. (2022). Mechanisms controlling carbon sinks in semi‐arid mountain ecosystems. *Global Biogeochemical Cycles*, e2021GB007186.

Gustafsson, J. E., & Martenson, R. (2002). Structural equation modeling with AMOS: Basic concepts, applications, and programming. In: Contemporary Psychology-Apa Review of Books, 478–480.

Hagedorn, F., Gavazov, K., & Alexander, J. M. (2019). Above-and belowground linkages shape responses of mountain vegetation to climate change. *Science*, **365**(6458), 1119–1123.

Harmon, M. E., Fasth, B. G., Yatskov, M., Kastendick, D., Rock, J., & Woodall, C. W. (2020). Release of coarse woody detritus-related carbon: a synthesis across forest biomes. *Carbon Balance and Management*, **15**(1), 1–21.

Harris, N. L., Gibbs, D. A., Baccini, A., Birdsey, R. A., De Bruin, S., Farina, M., et al. (2021). Global maps of twenty-first century forest carbon fluxes. *Nature Climate Change*, **11**(3), 234–240.

Hart, S. C., Firestone, M. K., & Paul, E. A. (1992). Decomposition and nutrient dynamics of ponderosa pine needles in a Mediterranean-type climate. *Canadian Journal of Forest Research*, **22**(3), 306–314.

Hasenmueller, E. A., Gu, X., Weitzman, J. N., Adams, T. S., Stinchcomb, G. E., Eissenstat, D. M., et al. (2017). Weathering of rock to regolith: The activity of deep roots in bedrock fractures. *Geoderma*, **300**, 11–31.

He, X., Hou, E., Liu, Y., & Wen, D. (2016). Altitudinal patterns and controls of plant and soil nutrient concentrations and stoichiometry in subtropical China. *Scientific Reports*, **6**(1), 1–9.

Hicks Pries, C. E., Castanha, C., Porras, R. C., & Torn, M. S. (2017). The whole-soil carbon flux in response to warming. *Science*, **355**(6332), 1420–1423.

Holbrook, W. S., Riebe, C. S., Elwaseif, M., L. Hayes, J., Basler-Reeder, K., L. Harry, D., et al. (2014). Geophysical constraints on deep weathering and water storage potential in the Southern Sierra Critical Zone Observatory. *Earth Surface Processes and Landforms*, **39**(3), 366–380.

Hou, E., Chen, C., Luo, Y., Zhou, G., Kuang, Y., Zhang, Y., et al. (2018). Effects of climate on soil phosphorus cycle and availability in natural terrestrial ecosystems. *Global Change Biology*, **24**(8), 3344–3356.

Hunsaker, C. T., Whitaker, T. W., & Bales, R. C. (2012). Snowmelt runoff and water yield along elevation and temperature gradients in California's southern Sierra Nevada. *Journal of the American Water Resources Association*, **48**(4), 667–678.

Jenkins, J. C., Chojnacky, D. C., Heath, L. S., & Birdsey, R. A. (2003). National-scale biomass estimators for United States tree species. *Forest Science*, **49**(1), 12–35.

Jia, J., Cao, Z., Liu, C., Zhang, Z., Lin, L. I., Wang, Y., et al. (2019). Climate warming alters subsoil but not topsoil carbon dynamics in alpine grassland. *Global Change Biology*, **25**(12), 4383–4393.

Jobbágy, E. G., & Jackson, R. B. (2000). The vertical distribution of soil organic carbon and its relation to climate and vegetation. *Ecological Applications*, **10**(2), 423–436.

Johnson, D. W., Hunsaker, C. T., Glass, D. W., Rau, B. M., & Roath, B. A. (2011). Carbon and nutrient contents in soils from the Kings River Experimental Watersheds, Sierra Nevada Mountains, California. *Geoderma*, **160**(3-4), 490–502.

Kaye, J. P., Hart, S. C., Fulé, P. Z., Covington, W. W., Moore, M. M., & Kaye, M. W. (2005). Initial carbon, nitrogen, and phosphorus fluxes following ponderosa pine restoration treatments. *Ecological Applications*, **15**(5), 1581–1593.

Kelly, A. E. (2014). Climate controls on ecosystem production, biomass, and water cycling. (Doctoral dissertation). Retrieved from [ProQuest]. (https://czo-archive.criticalzone.org/sierra/publications/pub/kelly-2014-climate-controls-on-ecosystem-production-biomass-and-water-cycli/) Location: University of California, Irvine.

Kelly, A. E., & Goulden, M. L. (2008). Rapid shifts in plant distribution with recent climate change. *Proceedings of the National Academy of Sciences*, **105**(33), 11823–11826.

Kelly, A. E., & Goulden, M. L. (2016). A montane Mediterranean climate supports year-round photosynthesis and high forest biomass. *Tree Physiology*, **36**(4), 459–468.

Klos, P. Z., Goulden, M. L., Riebe, C. S., Tague, C. L., O'Geen, A. T., Flinchum, B. A., et al. (2018). Subsurface plant-accessible water in mountain ecosystems with a Mediterranean climate. *Wiley Interdisciplinary Reviews: Water*, **5**(3), e1277.

Körner, C. (2007). The use of 'elevation' in ecological research. *Trends in ecology & evolution*, **22**(11), 569–574.

Lajtha, K., Driscoll, C. T., Jarrell, W. M., & Elliott, E. T. (1999). Soil Phosphorus Characterization and Total Element Analysis, in: Robinson GP, Coleman DC, Bledsoe CS, Sollins P (Eds.), Standard Soil Methods for Ecological Research. Oxford University Press., New York, 115–142.

Laudenslayer, W. F., & Darr, H. H. (1990). Historical effects of logging on forests of the Cascade and Sierra Nevada Ranges of California. *1990 Transactions of the Western Section of the Wildlife Society*, **26**, 12–23.

Li, J., Pei, J., Pendall, E., Reich, P. B., Noh, N. J., Li, B., et al. (2020). Rising temperature may trigger deep soil carbon loss across forest ecosystems. *Advanced Science*, **7**(19), 2001242.

Lionello, P. (2012). The Climate of the Mediterranean Region: From the Past to the Future. *The Climate of the Mediterranean Region* (Elsevier), https://doi.org/10.1016/b978-0-12-416042-2.00011-2.

Lionello, P., & Scarascia, L. (2018). The relation between climate change in the Mediterranean region and global warming. *Regional Environmental Change*, **18**(5), 1481–1493.

Liu, N., & Nan, H. (2018). Carbon stocks of three secondary coniferous forests along an altitudinal gradient on Loess Plateau in inland China. *PloS one*, **13**(5), e0196927.

Lu, M., Zhou, X., Yang, Q., Li, H., Luo, Y., Fang, C., et al. (2013). Responses of ecosystem carbon cycle to experimental warming: a meta-analysis. *Ecology*, **94**(3), 726–738.

Lund, J., Medellin-Azuara, J., Durand, J., & Stone, K. (2018). Lessons from California's 2012–2016 drought. *Journal of Water Resources Planning and Management*, **144**(10), 04018067.

Luo, Y., Gerten, D., Le Maire, G., Parton, W. J., Weng, E., Zhou, X., et al. (2008). Modeled interactive effects of precipitation, temperature, and [CO_2] on ecosystem carbon and water dynamics in different climatic zones. *Global Change Biology*, **14**(9), 1986–1999.

Ma, M., & Chang, R. (2019). Temperature drive the altitudinal change in soil carbon and nitrogen of montane forests: Implication for global warming. *Catena*, **182**, 104126.

Maaroufi, N. I., & De Long, J. R. (2020). Global change impacts on forest soils: linkage between soil biota and carbon-nitrogen-phosphorus stoichiometry. *Frontiers in Forests and Global Change*, **3**, 16.

Marin-Spiotta, E., Chadwick, O. A., Kramer, M., & Carbone, M. S. (2011). Carbon delivery to deep mineral horizons in Hawaiian rain forest soils. *Journal of Geophysical Research: Biogeosciences*, **116**, G03011.

Matchett, J. R., Lutz, J. A., Tarnay, L. W., Smith, D. G., Becker, K. M., & Brooks, M. L. (2015). Impacts of fire management on aboveground tree carbon stocks in Yosemite and Sequoia & Kings Canyon National Parks, Natural Resource Report NPS/SIEN/NRR—2015/910, Fort Collins, Colorado, Retrieved from http://pubs.er.usgs.gov/publication/70140618.

Mattson, K. G., & Zhang, J. (2019). Forests in the northern Sierra Nevada of California, USA, store large amounts of carbon in different patterns. *Ecosphere*, **10**(6), e02778.

Maxwell, T. M., Silva, L. C., & Horwath, W. R. (2018). Integrating effects of species composition and soil properties to predict shifts in montane forest carbon–water relations. *Proceedings of the National Academy of Sciences*, **115**(18), E4219–E4226.

McGill, W. B., & Cole, C. V. (1981). Comparative aspects of cycling of organic C, N, S and P through soil organic matter. *Geoderma*, **26**(4), 267–286.

Melillo, J. M., Butler, S., Johnson, J., Mohan, J., Steudler, P., Lux, H., et al. (2011). Soil warming, carbon–nitrogen interactions, and forest carbon budgets. *Proceedings of the National Academy of Sciences*, **108**(23), 9508–9512.

Melillo, J. M., Frey, S. D., DeAngelis, K. M., Werner, W. J., Bernard, M. J., Bowles, F. P., et al. (2017). Long-term pattern and magnitude of soil carbon feedback to the climate system in a warming world. *Science*, **358**(6359), 101–105.

Miesel, J. R. (2012). Differential responses of Pinus ponderosa and Abies concolor foliar characteristics and diameter growth to thinning and prescribed fire treatments. *Forest Ecology and Management*, **284**, 163–173.

Minocha, R., Turlapati, S. A., Long, S., & North, M. (2013). Fuel treatment effects on soil chemistry and foliar physiology of three coniferous species at the Teakettle Experimental Forest, California, USA. *Trees*, **27**(4), 1101–1113.

Moreland, K., Tian, Z., Berhe, A. A., McFarlane, K. J., Hartsough, P., Hart, S. C., et al. (2021). Deep in the Sierra Nevada critical zone: saprock represents a large terrestrial organic carbon stock. *Environmental Research Letters*, **16**(12), 124059.

Moreland, K. C. (2020). Climatic Controls on Deep Soil Carbon and Nitrogen Dynamics. (Doctoral dissertation). Retrieved from [ProQuest]. (https://www.proquest.com/openview/1b58d05fa764e641ef7880224e485bbd/1?pq-origsite=gscholar&cbl=18750&diss=y) Location: University of California, Merced.

Moser, G., Leuschner, C., Hertel, D., Graefe, S., Soethe, N., & Iost, S. (2011). Elevation effects on the carbon budget of tropical mountain forests (S Ecuador): the role of the belowground compartment. *Global Change Biology*, **17**(6), 2211–2226.

Neumann, M., Ukonmaanaho, L., Johnson, J., Benham, S., Vesterdal, L., Novotný, R., et al. (2018). Quantifying carbon and nutrient input from litterfall in European forests using field observations and modeling. *Global Biogeochemical Cycles*, **32**(5), 784–798.

O'Geen, A., Safeeq, M., Wagenbrenner, J., Stacy, E., Hartsough, P., Devine, S., et al. (2018). Southern Sierra Critical Zone Observatory and Kings River Experimental Watersheds: A synthesis of measurements, new insights, and future directions. *Vadose Zone Journal*, **17**(1), 1–18.

Pan, Y., Birdsey, R. A., Fang, J., Houghton, R., Kauppi, P. E., Kurz, W. A., et al. (2011). A large and persistent carbon sink in the world's forests. *Science*, **333**(6045), 988–993.

Paz-Kagan, T., Brodrick, P. G., Vaughn, N. R., Das, A. J., Stephenson, N. L., Nydick, K. R., & Asner, G. P. (2017). What mediates tree mortality during drought in the southern Sierra Nevada?. *Ecological Applications*, **27**(8), 2443–2457.

Pearson, J. A., Knight, D. H., & Fahey, T. J. (1987). Biomass and nutrient accumulation during stand development in Wyoming lodgepole pine forests. *Ecology*, **68**(6), 1966–1973.

Pickett, S.T.A. (1989) Space-for-time substitution as an alternative to long-term studies. In: Likens G.E. (eds) Long-Term Studies in Ecology (pp. 110-135). Springer, New York, NY. https://doi.org/10.1007/978-1-4615-7358-6_5

Powers, R. F. (1979). Response of California true fir to fertilization. *In Proceedings of Forest Fertilization Conference* (pp. 24-25), http://apps.sefs.uw.edu/research.smc/RFNRP/1FFC_Powers1.pdf.

Prichard, S. J., Hessburg, P. F., Hagmann, R. K., Povak, N. A., Dobrowski, S. Z., Hurteau, M. D., et al. (2021). Adapting western North American forests to climate change and wildfires: 10 common questions. *Ecological Applications*, **0**, e02433.

Pries, C., Heckman, K., Templer, P., Frey, S., & Crow, S. (2021). The response of deep soil carbon to climate change: From experiments to meta-analysis. In EGU General Assembly Conference Abstracts (pp. EGU21-16152). https://doi.org/10.5194/egusphere-egu21-16152.

Raich, J. W., Russell, A. E., Kitayama, K., Parton, W. J., & Vitousek, P. M. (2006). Temperature influences carbon accumulation in moist tropical forests. *Ecology*, **87**(1), 76–87.

Reed, C. C., & Hood, S. M. (2021). Few generalizable patterns of tree-level mortality during extreme drought and concurrent bark beetle outbreaks. *Science of the Total Environment*, **750**, 141306.

Richter, D. D., Hofmockel, M., Callaham, M. A., Powlson, D. S., & Smith, P. (2007). Long-term soil experiments: Keys to managing Earth's rapidly changing ecosystems. *Soil Science Society of America Journal*, **71**(2), 266–279.

Rick, T., Ontiveros, M. Á. C., Jerardino, A., Mariotti, A., Méndez, C., & Williams, A. N. (2020). Human-environmental interactions in Mediterranean climate regions from the Pleistocene to the Anthropocene. *Anthropocene*, **31**, 100253.

Robeson, S. M. (2015). Revisiting the recent California drought as an extreme value. *Geophysical Research Letters*, **42**(16), 6771–6779.

Rumpel, C., & Kögel-Knabner, I. (2011). Deep soil organic matter-a key but poorly understood component of terrestrial C cycle. *Plant and Soil*, **338**(1), 143–158.

Rumpf, S. B., Hülber, K., Klonner, G., Moser, D., Schütz, M., Wessely, J., et al. (2018). Range dynamics of mountain plants decrease with elevation. *Proceedings of the National Academy of Sciences*, **115**(8), 1848–1853.

Rundel, P. W., St.John, T. V., & Westman, W. (1985). Vegetation process studies, Log Meadow, Sequoia National Park. *California Air Resources Board Integrated Watershed Project Final Contract Report A3-097-32*. https://ww2.arb.ca.gov/sites/default/files/classic/research/apr/past/a3-097-32a.pdf.

Rustad, L. E. J. L., Campbell, J., Marion, G., Norby, R., Mitchell, M., Hartley, A., et al. (2001). A meta-analysis of the response of soil respiration, net nitrogen mineralization, and aboveground plant growth to experimental ecosystem warming. *Oecologia*, **126**(4), 543–562.

Santiago, L. S., Kitajima, K., Wright, S. J., & Mulkey, S. S. (2004). Coordinated changes in photosynthesis, water relations and leaf nutritional traits of canopy trees along a precipitation gradient in lowland tropical forest. *Oecologia*, **139**(4), 495–502.

Santiago, L. S., Schuur, E. A., & Silvera, K. (2005). Nutrient cycling and plant-soil feedbacks along a precipitation gradient in lowland Panama. *Journal of Tropical Ecology*, **21**(4), 461–470.

Schlesinger, W. H., & Andrews, J. A. (2000). Soil respiration and the global carbon cycle. *Biogeochemistry*, **48**(1), 7–20.

Schwartz, M. W., Butt, N., Dolanc, C. R., Holguin, A., Moritz, M. A., North, M. P., et al. (2015). Increasing elevation of fire in the Sierra Nevada and implications for forest change. *Ecosphere*, **6**(7), 1–10.

Seager, R., Osborn, T. J., Kushnir, Y., Simpson, I. R., Nakamura, J., & Liu, H. (2019). Climate variability and change of Mediterranean-type climates. *Journal of Climate*, **32**(10), 2887–2915.

Selmants, P. C., Litton, C. M., Giardina, C. P., & Asner, G. P. (2014). Ecosystem carbon storage does not vary with mean annual temperature in Hawaiian tropical montane wet forests. *Global Change Biology*, **20**(9), 2927–2937.

Serrano-Ortiz, P., Were, A., Reverter, B. R., Villagarcía, L., Domingo, F., Dolman, A. J., & Kowalski, A. S. (2015). Seasonality of net carbon exchanges of Mediterranean ecosystems across an altitudinal gradient. *Journal of Arid Environments*, **115**, 1–9.

Siyum, Z. G. (2020). Tropical dry forest dynamics in the context of climate change: syntheses of drivers, gaps, and management perspectives. *Ecological Processes*, **9**, 1–16.

Song, B., Niu, S., Zhang, Z., Yang, H., Li, L., & Wan, S. (2012). Light and heavy fractions of soil organic matter in response to climate warming and increased precipitation in a temperate steppe. *PloS one*, **7**(3), e33217.

Soong, J. L., Castanha, C., Hicks Pries, C. E., Ofiti, N., Porras, R. C., Riley, W. J., et al. (2021). Five years of whole-soil warming led to loss of subsoil carbon stocks and increased CO_2 efflux. *Science advances*, **7**(21), eabd1343.

Stacy, E. M., Hart, S. C., Hunsaker, C. T., Johnson, D. W., & Berhe, A. A. (2015). Soil carbon and nitrogen erosion in forested catchments: implications for erosion-induced terrestrial carbon sequestration. *Biogeosciences*, **12**(16), 4861–4874.

Steinbauer, M. J., Grytnes, J. A., Jurasinski, G., Kulonen, A., Lenoir, J., Pauli, H., et al. (2018). Accelerated increase in plant species richness on mountain summits is linked to warming. *Nature*, **556**(7700), 231–234.

Sun, X., Tang, Z., Ryan, M. G., You, Y., & Sun, O. J. (2019). Changes in soil organic carbon contents and fractionations of forests along a climatic gradient in China. *Forest Ecosystems*, **6**(1), 1–12.

Tan, Q., & Wang, G. (2016). Decoupling of nutrient element cycles in soil and plants across an altitude gradient. *Scientific Reports*, **6**(1), 1–9.

Tashi, S., Singh, B., Keitel, C., & Adams, M. (2016). Soil carbon and nitrogen stocks in forests along an altitudinal gradient in the eastern Himalayas and a meta-analysis of global data. *Global Change Biology*, **22**(6), 2255–2268.

Terrer, C., Jackson, R. B., Prentice, I. C., Keenan, T. F., Kaiser, C., Vicca, S., et al. (2019). Nitrogen and phosphorus constrain the CO 2 fertilization of global plant biomass. *Nature Climate Change*, **9**(9), 684–689.

Thomas, G. W., & Sparks, D. L. (1996). Methods of Soil Analysis, Part 3-Chemical Methods. Soil pH and soil acidity. (J.M. Bigham., pp. 475–490). Madison, WI, USA: Soil Science Society of America, American Society of Agronomy.

Tian, Z., Hartsough, P. C., & O'Geen, A. T. (2019). Lithologic, climatic and depth controls on critical zone transformations. *Soil Science Society of America Journal*, **83**(2), 437–447.

Tiedemann, A. R., & Clary, W. P. (1996). Nutrient distribution in *Quercus gambelii* stands in central Utah. *The Great Basin Naturalist*, **56**(2), 119–128.

Todd-Brown, K. E. O., Randerson, J. T., Post, W. M., Hoffman, F. M., Tarnocai, C., Schuur, E. A. G., & Allison, S. D. (2013). Causes of variation in soil carbon simulations from CMIP5 Earth system models and comparison with observations. *Biogeosciences*, **10**(3), 1717–1736.

Tsozué, D., Nghonda, J. P., Tematio, P., & Basga, S. D. (2019). Changes in soil properties and soil organic carbon stocks along an elevation gradient at Mount Bambouto, Central Africa. *Catena*, **175**, 251–262.

Turnipseed, A. A., Blanken, P. D., Anderson, D. E., & Monson, R. K. (2002). Energy budget above a high-elevation subalpine forest in complex topography. Agricultural and Forest Meteorology, 110(3), 177–201.

Turnipseed, A. A., Anderson, D. E., Blanken, P. D., Baugh, W. M., & Monson, R. K. (2003). Airflows and turbulent flux measurements in mountainous terrain: Part 1. Canopy and local effects. Agricultural and Forest Meteorology, 119(1-2), 1–21.

Unger, M., Homeier, J., & Leuschner, C. (2012). Effects of soil chemistry on tropical forest biomass and productivity at different elevations in the equatorial Andes. *Oecologia*, **170**(1), 263–274.

van der Molen, M. K., Dolman, A. J., Ciais, P., Eglin, T., Gobron, N., Law, B. E., et al. (2011). Drought and ecosystem carbon cycling. *Agricultural and Forest Meteorology*, **151**(7), 765–773.

Vieira, S. A., Alves, L. F., Duarte-Neto, P. J., Martins, S. C., Veiga, L. G., Scaranello, M. A., et al. (2011). Stocks of carbon and nitrogen and partitioning between above- and belowground pools in the Brazilian coastal Atlantic Forest elevation range. *Ecology and Evolution*, **1**(3), 421–434.

Walker, T. W., & Syers, J. K. (1976). The fate of phosphorus during pedogenesis. *Geoderma*, **15**(1), 1–19.

Wang, Y., Amundson, R., & Niu, X. F. (2000). Seasonal and altitudinal variation in decomposition of soil organic matter inferred from radiocarbon measurements of soil CO_2 flux. *Global Biogeochemical Cycles*, **14**(1), 199–211.

Williams, A. P., Cook, E. R., Smerdon, J. E., Cook, B. I., Abatzoglou, J. T., Bolles, K., et al. (2020). Large contribution from anthropogenic warming to an emerging North American megadrought. *Science*, **368**(6488), 314–318.

Wood, T., Bormann, F. H., & Voigt, G. K. (1984). Phosphorus cycling in a northern hardwood forest: biological and chemical control. *Science*, **223**(4634), 391–393.

Woodall, C. W., Fraver, S., Oswalt, S. N., Goeking, S., Domke, G., & Russell, M. (2021). Decadal dead wood biomass dynamics of coterminous US forests. *Environmental Research Letters*, **16**, 104034.

Woodmansee, R. G., & Duncan, D. A. (1980). Nitrogen and phosphorus dynamics and budgets in annual grasslands. *Ecology*, **61**(4), 893–904.

Yan, Y., Zhou, X., Jiang, L., & Luo, Y. (2017). Effects of carbon turnover time on terrestrial ecosystem carbon storage. *Biogeosciences*, **14**(23), 5441–5454.

Yang, Y., Yanai, R. D., See, C. R., & Arthur, M. A. (2017). Sampling effort and uncertainty in leaf litterfall mass and nutrient flux in northern hardwood forests. *Ecosphere*, **8**(11), e01999.

Yang, Y., Berhe, A. A., Hunsaker, C. T., Johnson, D. W., Safeeq, M., Barnes, M. E., et al. (2022). Impacts of climate and disturbance on nutrient fluxes and stoichiometry in mixed-conifer forests. *Biogeochemistry*, **158**(1), 1-20.

Zhang, H., Wang, E., Zhou, D., Luo, Z., & Zhang, Z. (2016). Rising soil temperature in China and its potential ecological impact. *Scientific Reports*, **6**(1), 1–8.

Ziegler, S. E., Benner, R., Billings, S. A., Edwards, K. A., Philben, M., Zhu, X., & Laganière, J. (2017). Climate warming can accelerate carbon fluxes without changing soil carbon stocks. *Frontiers in Earth Science*, **5**, 2.

Phillips, J., Ramirez, S., Wayson, C., & Duque, A. (2019). Differences in carbon stocks along an elevational gradient in tropical mountain forests of Colombia. *Biotropica*, **51**(4), 490–499.

Figure Captions

Figure 1. The conceptual diagram (left), representative site pictures (central), and location and climatic values (right) of Southern Sierra Critical Zone Observatory bioclimatic gradient on the western slope of the Sierra Nevada, California, USA. The four sites consist of oak savannah (elevation 405 m.a.s.l.), pine-oak forest (1160 m), mixed-conifer forest (2015 m), and subalpine forest (2700 m). The pine-oak and mixed-conifer forest at mid elevations receive a more favorable climate (not too dry or too hot) compared to the oak savannah and the subalpine forest at lower and higher elevations, respectively, which results in thicker regolith profile (soil + weathered bedrock) and denser vegetation (shown in the conceptual diagram). Regolith thickness in this study was ~1.6 m in oak savannah, ~4.2 m in the pine-oak forest, ~9.5 m in the mixed-conifer forest, and ~1.0 m in the subalpine forest. The mean annual air temperatures (MAAT) and mean annual precipitation amount (MAP) were estimated based on period of record 1970 – 2020 (PRISM; https://www.prism.oregonstate.edu/).

Figure 2. Gross primary productivity (GPP), net ecosystem productivity (NEP), and ecosystem respiration rate (ER) along the Southern Sierra Critical Zone Observatory bioclimatic gradient, California, USA. The four sites consist of oak savannah (elevation 405 m.a.s.l.), pine-oak forest (1160 m), mixed-conifer forest (2015 m), and subalpine forest (2700 m). Measurements were based on one eddy covariance flux tower situated at each of the four sites (https://www.ess.uci.edu/~california/). Error bars are the standard error of three replicated years prior to drought (water year 2010 – 2012; not shown if smaller than the symbol). Stylized trends with elevation are shown based on optimal regression models (linear for ER and quadratic for GPP and NEP).

Figure 3. Litterfall fluxes and vegetation and regolith stocks of carbon (C, a-c), nitrogen (N, d-f), and phosphorus (P, g-i) along the Southern Sierra Critical Zone Observatory bioclimatic gradient, California, USA. The four sites consist of oak savannah (elevation 405 m.a.s.l.), pine-oak forest (1160 m), mixed-conifer forest (2015 m), and subalpine forest (2700 m). Error bars for litterfall nutrient fluxes were the standard error of replicated years (n = 2 or 3 depending on site). Error bars for regolith nutrient stocks were propagated from the individual standard errors for each horizon of 4 replicate soil pits. Error bars smaller than the symbol are not shown. Panel c, f, and i are stylized trends with elevation and associated statistics for nutrient stocks based on a regression model, either linear or quadratic (selected based on the Akaike information criterion corrected for small sample sizes). One-way ANOVAs with Tukey's Honestly Significant Difference was used to examine differences among sites (indicated by different lower case letters), except for plant nutrient stocks where values were estimated once in 2009 and 2010 for the whole one-ha plot per site (i.e., no replicates across space and time and hence no error bars). The oak savannah site did not have an O horizon (i.e., forest floor), and P stock in O horizons were negligible compared to total regolith P stock at the other sites (< 1% of total soil P stock).

Figure 4. Climatic impacts and the corresponding standardized total impact (unitless) on regolith carbon (C) stock according to path analyses for the entire regolith profile (a and b), A horizons (c and d), B horizons (e and f), and saprock horizons (g and h) along the Southern Sierra Critical Zone Observatory bioclimatic gradient, California, USA. Climatic variables were mean annual precipitation (MAP) and mean annual air temperature (MAAT). Indirect impacts of climate are indicated by the influences of regolith properties on regolith C stock. Regolith properties included % clay, % silt, pH_{CaCl_2}, and stocks of

nitrogen (N) and phosphorus (P) in each horizon. Goodness-of-fit statistics were χ^2/df = 3.42, RMSEA = 0.41 for whole regolith profiles, χ^2/df = 3.77, RMSEA = 0.42 for the A horizons, χ^2/df = 3.83, RMSEA = 0.43 for the B horizons, and χ^2/df = 3.42, RMSEA = 0.40 for the saprock horizons. In the four path analysis diagrams, red and blue arrows indicated significantly ($p < 0.10$) positive and negative influences, respectively; black arrows were non-significant relationships. The widths of red and blue arrows are proportional to the strength of standardized path coefficients.

Figure 5. Linear correlations among climatic variables, regolith properties, overstory carbon (C) stock, and productivity variables along the Southern Sierra Critical Zone Observatory bioclimatic gradient, California, USA. Climatic variables were mean annual precipitation (MAP) and mean annual air temperature (MAAT). Regolith properties were mean % clay, % silt, and pH_{CaCl_2}, and total regolith stocks of C, nitrogen (N), and phosphorus (P). Mean % clay, % silt, pH_{CaCl_2} were averages across mineral soil and saprock horizons and pits, and weighted by bulk density, thickness, and rock fraction. Productivity variables were gross primary productivity (GPP), net ecosystem productivity (NEP), ecosystem respiration rate (ER), and litterfall C flux. Correlation coefficients were estimated using Pearson correlation tests (n = 4 sites) and colored based on their magnitudes and directions. Bolded values were statistically significant, and lighter values were not ($\alpha = 0.10$).

Figure 6. Changes in mean residence time (MRT) of ecosystem carbon (C) along the Southern Sierra Critical Zone Observatory bioclimatic gradient, California, USA. The four sites consist of oak savannah (elevation 405 m.a.s.l.), pine-oak forest (1160 m), mixed-conifer forest (2015 m), and subalpine forest (2700 m). Different MRT estimates were generated using different combinations of C stocks within a given site, divided by the same pre-drought gross primary productivity (all assuming steady-state conditions). Different combinations of C stocks included: overstory biomass, overstory biomass plus the O horizon, overstory biomass plus the O + A horizons, overstory biomass plus the O + A + B horizons, and overstory biomass plus the O + A + B + saprock horizons). The oak savannah site did not have an O horizon.

Figure 7. Projected percent changes in overstory carbon (C) stock, total regolith C stock, gross primary productivity, and mean residence time (MRT) of ecosystem C under a modeled increase in mean annual air temperature of 0.5 and 1.0 °C in the oak savannah (a), pine-oak forest (b), mixed-conifer forest (c), and subalpine forest (d) at the Southern Sierra Critical Zone Observatory bioclimatic gradient in California, USA. The MRT of ecosystem C is defined as the average time that a C atom resides within the ecosystem from initial photosynthetic fixation until loss from the ecosystem primarily by respiration, and is calculated as the ratio of C stock in overstory biomass and the entire regolith (soil + saprock) to gross primary productivity assuming that ecosystem C is in steady-state. Values in red inside each panel were the absolute changes in MRT of ecosystem C under projected increases in the mean annual air temperature at each site.

Figure 8. Percent changes in gross primary productivity, ecosystem carbon (C) stock (overstory and whole-regolith profile), and mean residence time (MRT) of ecosystem C (panel a), and the overstory C stock prior to (2009 – 2010) and following a major drought event (2016 – 2017; panel b) along the Southern Sierra Critical Zone Observatory bioclimatic gradient in California, USA. The four sites consist of oak savannah (elevation 405 m.a.s.l.), pine-oak forest (1160 m), mixed-conifer forest (2015 m), and

subalpine forest (2700 m). Carbon stock in live trees following drought was calculated based on the remaining trees by applying the percent dead trees observed at nearby sites from the literature to our tree inventory prior to drought (Figure S5 and S6 in Supporting Information S1 and Table S3 in Supporting Information S2). Absolute changes in MRT of ecosystem C following drought were indicated by values in red inside panel a.

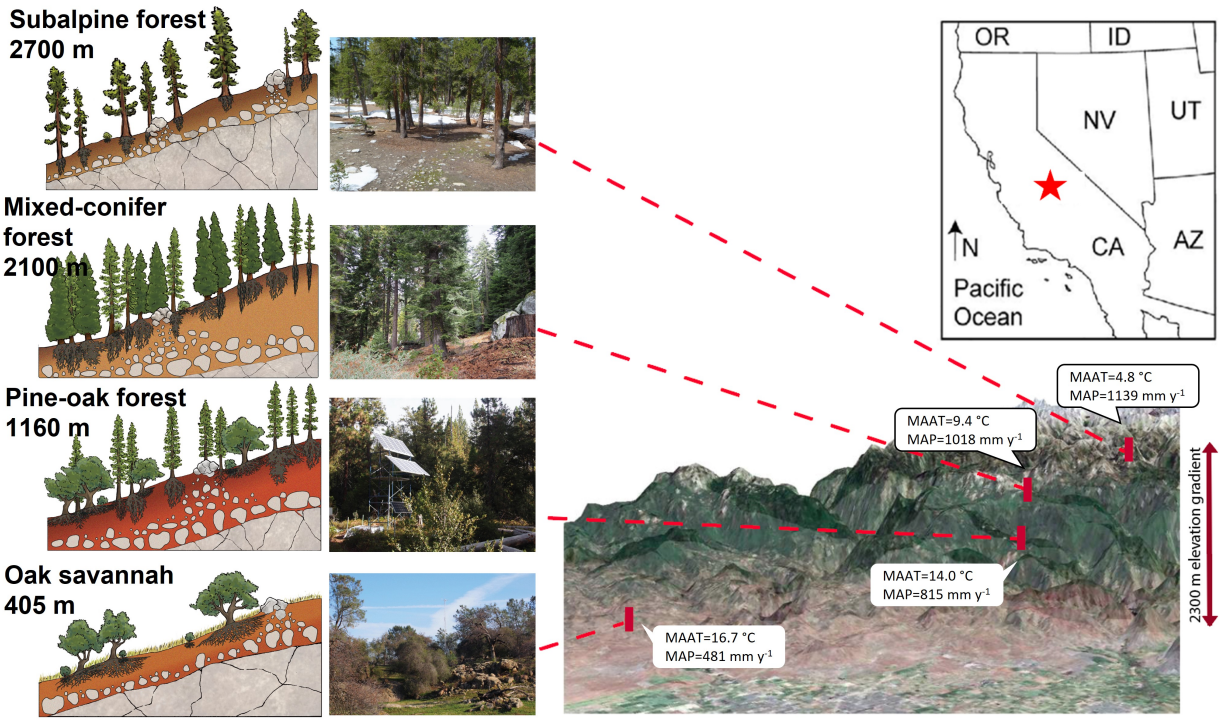

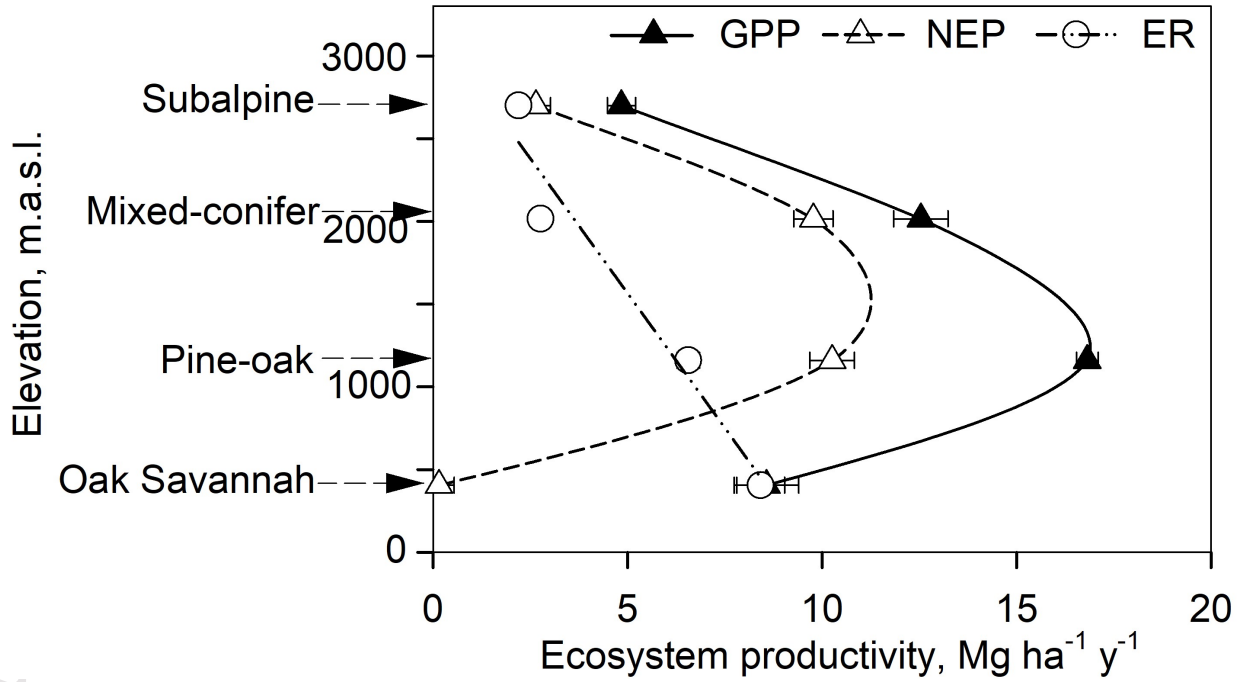

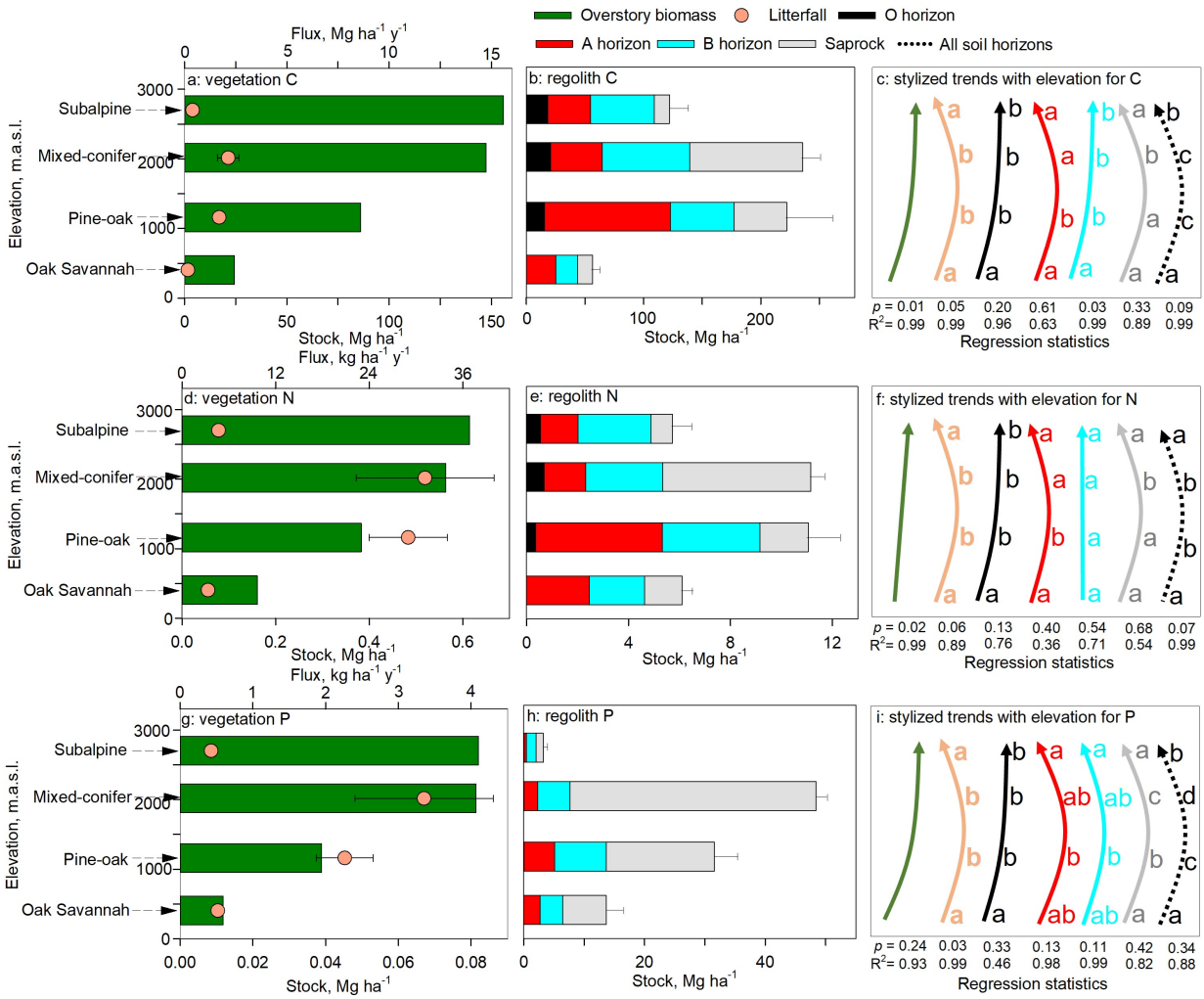

a) Path analysis for the entire regolith profile

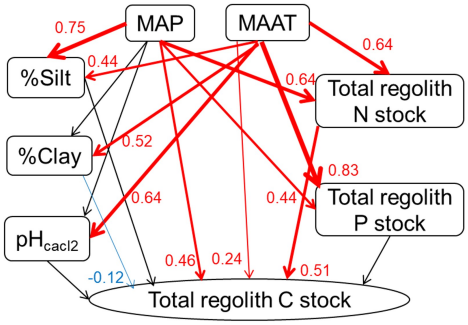

b) Standardized total impact on C stock in the entire regolith profile

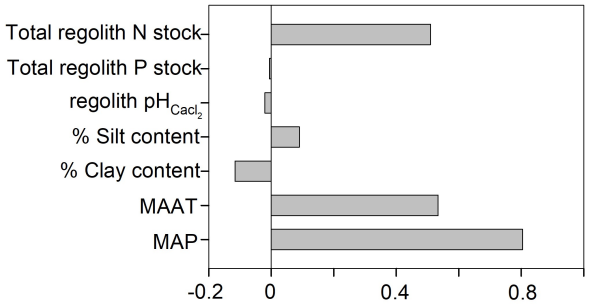

c) Path analysis in A horizons

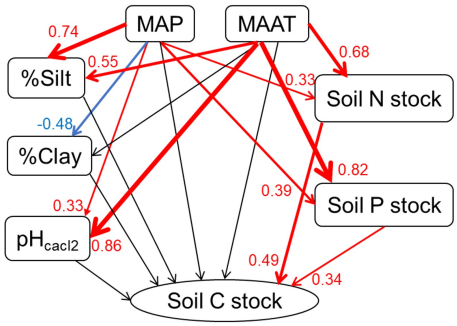

d) Standardized total impact on C stock in A horizons

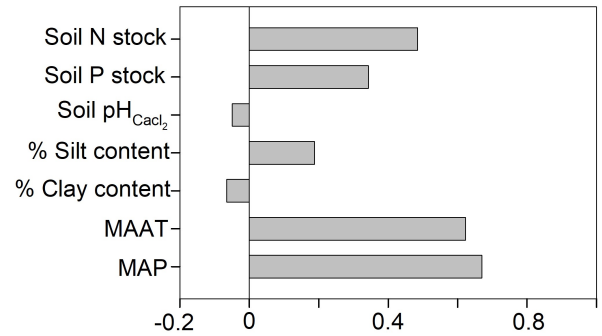

e) Path analysis in B horizons

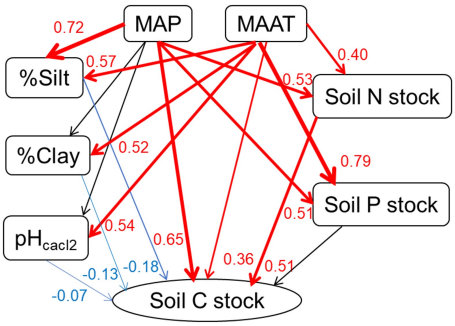

f) Standardized total impact on C stock in B horizons

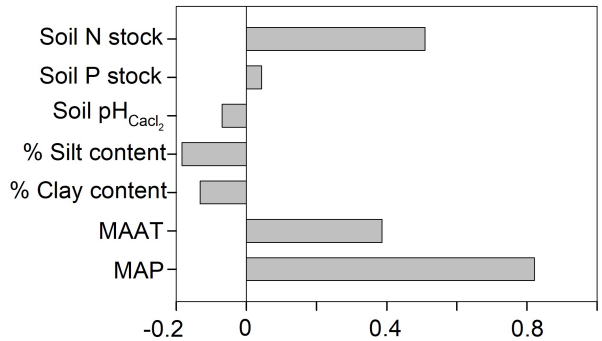

g) Path analysis in saprock horizons

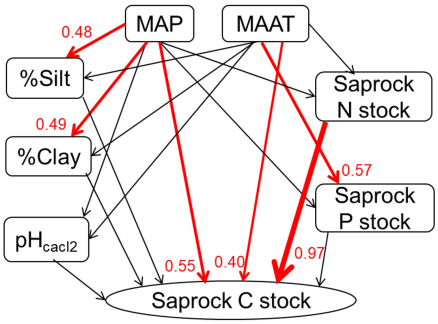

h) Standardized total impact on C stock in saprock horizons